Article

Not peer-reviewed version

Elevated Growth Temperature Reduced the Physiological Plasticity of *Fagus sylvatica* Seedlings in Response to Drought and Shade

Faustino Rubio *, Ismael Aranda, Rosana López, Francisco Javier Cano *

Posted Date: 22 April 2025

doi: 10.20944/preprints202504.1808.v1

Keywords: drought; high temperature; shade; anatomy; hydraulics; coordination; trade-offs; phenotypic plasticity; leaf gas exchange; PV curves

 doi:10.20944/preprints202504.1808.v1

Article

Elevated Growth Temperature Reduced the Physiological Plasticity of *Fagus sylvatica* Seedlings in Response to Drought and Shade

Faustino Rubio [1,*], Ismael Aranda [2], Rosana López [1] and Francisco Javier Cano [2,3,*]

[1] Departamento de Sistemas y Recursos Naturales, Escuela Técnica Superior de Ingeniería de Montes, Forestal y del Medio Natural, Universidad Politécnica de Madrid, Madrid 28040, Spain

[2] Instituto de Ciencias Forestales (ICIFOR-INIA), CSIC, Madrid, Spain

[3] Hawkesbury Institute for the Environment, Western Sydney University, Richmond, NSW, Australia

* Correspondence: FR: faustino.rubio.perez@upm.es; Tel.: +34 686574658 & FCJ: javier.cano@inia.csic.es; Tel.: +34 913476784

Abstract: Climate change is increasing the growing temperature worldwide, adding a potential new stress factor to those already present during the regeneration phase of many tree species, particularly late successional species: water deficit and shade. We performed a multifactorial stress experiment by rising the growing temperature above optimum (25°C and +7.5°C) without elevating vapor pressure deficit (VPD), long-term water deficit or well-watered and high and low light intensity, and measured plant growth, leaf gas exchange and water relations and hydraulic traits on one year-old beech seedlings. Many functional traits showed synergies across treatments (e.g. stem growth and net photosynthesis, total leaf area and vessel area, leaf transpiration and hydraulic conductivity). Warming decreased seedling's phenotypic plasticity. Plants under warmer growth temperatures showed lower midday water potential, water use efficiency, photosynthesis, leaf area and plant biomass but higher leaf transpiration, residual conductance and respiratory costs. When warming interacted with drought, gas exchange and the capacity to perform osmotic adjustment were severely affected, reducing the leaf safety margin and beech drought tolerance. Surprisingly, warming promoted a risky acquisitive strategy in shaded seedlings in well-watered plants, stimulating growth by increasing the number of less costly leaves. Global warming may compromise future regeneration of this shade-tolerant species under dry conditions.

Keywords: drought; high temperature; shade; anatomy; hydraulics; coordination; trade-offs; phenotypic plasticity; leaf gas exchange; PV curves

1. Introduction

The significant increase in temperature with ongoing climate change along with more frequent and severe droughts (e.g. scenario SSP5-8.5) [1] poses challenges for forest species, with long reproductive cycles, slow migration capacity, and yet unknown limits for acclimation to this scenario. Indeed, plant acclimation to warmer growing temperatures is an underexplored process, which gets even more complex when concurrent with other environmental stress factors. Many plant species face the triple interaction of growing under continuously rising temperatures, suffering events of water deficit, and regenerating in the light-limiting conditions of the understory [2,3]. To gain insights into how future warming will affect the regeneration niches of key late-successional species, as well as to understand how tree populations respond to rapid environmental changes, we need to study the phenotypic plasticity of essential functional traits in relation to these environmental stressors [4–6]. Changes in key functional traits may alter plant ecological strategies, such as drought and shade tolerance, which in turn may challenge the species' ability to compete at their regeneration niche and hence influence forest dynamics [7–9].

 doi:10.20944/preprints202504.1808.v1

The temperature response of most biological processes, such as metabolic and growth rates, follows an asymmetric Arrhenius equation, which present a maximum rate at the optimal temperature [10]. For example, warming can enhance tree growth and increase leaf area at the expense of root investment, particularly in deciduous temperate species as long as they are well-watered and fertilized. However, growth decreases once the optimal temperature for growth is exceeded. [11–13]. This decline is attributed to a reduction in plant leaf area and net photosynthesis (A_n) when the optimal temperature for the photosynthetic activity is exceeded [11,14,15]. Additionally, the rate of plant respiration continues to rise after reaching the optimum for An, further contributing to decreased growth [16]. A reduction in carbon availability is also shown by decreased leaf mass per area (*LMA*) with temperature [17]. *LMA* is a relevant trait of the leaf economical spectrum usually associated with plant ecological strategies, such as drought or shade tolerance [18,19]. Additionally, leaves are generally smaller when developed at elevated temperatures to reduce the boundary layer and facilitate heat dissipation [20–22]. Both photosynthesis (A_n) and respiration (R_d) acclimate to changes in growth temperature by the downregulation of respiration [16,23,24] and the upregulation of the temperature optimum for photosynthesis [12,23,25,26] which allows plants to maximize carbon gain with warming [27]. However, a decoupling between A_n and stomatal conductance (g_{sw}) at high temperature has been also reported in many species, particularly in warm adapted species, in a way that A_n decreases whereas g_{sw} increases due to the so-called evaporative cooling [28–32], with the concomitant reduction in intrinsic water use efficiency (iWUE) and enhancing the risk of dehydration [33].

The extent to which stomata acclimate to warming depends on a balance among their key functions. Stomata not only play a role in photosynthesis and contribute to the carbon economy, but they also regulate leaf water loss through the transpiration rate (*E*), leaf temperature through evaporative cooling [34], ROS-mediated impairment of normal metabolism [35] and leaf water potentials [36,37]. Maintaining these water potentials within specific safety limits is crucial to prevent hydraulic system failure [38] and leaf dehydration [39]. Leaf transpiration is the product of vapor pressure deficit from leaf to the atmosphere (VPD_L) multiplied by the total conductance for water vapor. Therefore, for the same stomatal aperture, more water is loss to the atmosphere when air temperature rises as consequence of elevated VPD_L [32,40]. To sustain higher water flow at higher evaporative demand, the leaf water potential at the turgor loss point (Ψ_{TLP}) usually decreases in seedlings grown at warmer temperatures [41], as often occurs with species or populations inhabiting warmer and dryer habitats [42,43], but it is still unknown if these adjustments occur in response to warming or to the interaction with other stressors such as low soil or air moisture [44].

Acclimation of the hydraulic architecture to warming in forest species remains understudied, even though it is expected to change since warmer climate increases the evaporative demand [12,41]. For example, well-watered *Populus tremuloides* seedlings grown at warmer temperatures than ambient showed higher growth, allocation to roots, which also increased their hydraulic conductance and the sapwood area to leaf area (Huber value, HV) [41]. However, in a xeric site, both *Juniperus monosperma* and *Pinus edulis* showed lack of acclimation of the HV or xylem anatomy after four years of atmospheric warming and only the juniper reduced its leaf specific hydraulic conductivity (K_L) associated with a decrease in canopy conductance under warming [40]. Well-watered plants grown under warmer conditions can develop larger and/or a more frequent conduits in the xylem [41,45,46], which may increase conductivity, but not necessarily affect embolism resistance. On the contrary, the vessel lumen of *Eucalyptus camaldulensis* and *E. grandis* was smaller, the specific conductivity (K_s) lower and wood density (W_D) higher when seedlings grew above optimum growth temperatures [47,48]. Besides changes in xylem anatomy, as the temperature increases, the density of sap remains more or less constant, but the viscosity decreases (i.e. lower resistance of water to motion) increasing whole plant hydraulic conductance just by the effect of sap temperature [47,49].

Warming increases the water deficit experienced by plants [50,51], but water deficit also exacerbates the negative effects of growing at supraoptimal temperature [52,53]. Water deficit reduces temperature optima for both photosynthesis, as consequence of reduced diffusional CO_2

 doi:10.20944/preprints202504.1808.v1

conductances [54,55], and tree growth due to the decreased photosynthesis rate, reduced production of leaf area and increased *LMA* [11]. However, an active osmotic adjustment shown in warmed trees can benefit drought tolerance [56]. Stomatal closure triggered by water deficit increases leaf temperature and, with it, the risk of tissue damage, even when thermal acclimation occurs [20,57]. When stomata are partially or fully closed as response to soil water deficit, water loss through the leaf cuticle becomes crucial for plant survival [58,59]. This leaf minimum conductance (g_{min}) usually decreases as consequence of drought, but high temperature during short time periods promotes the increase of g_{min} [60–62], although g_{min} may decrease over prolonged warmer temperatures due to the sustained higher VPD [33].

Another environmental stressor which hampers growth, and the regeneration capacity of many temperate tree species, is light availability [63,64]. In shaded conditions, plants allocate more resources to elongating stems and increasing leaf surface area to capture light [65–67], showing conflicting trade-offs with acclimation to water stress [68–73]. For example, lower capacity of osmotic adjustment of plants grown under shade [74–76], lower *LMA* [17] or lower biomass allocation to roots [77] can negatively affect the acclimation to drought and warmer temperatures. In contrast, large gaps in the forest expose seedlings to high light intensity and warmer temperatures, leading to increased metabolic activity and growth rates. However, these conditions also pose challenges such as heightened water stress and the risk of heat damage [20,78–82]. To understand the challenges that forest recruitment will face in a warmer world, we need to understand how elevated temperatures, water stress, and light conditions interact to affect plant performance. Additionally, it is important to recognize that the response of the stress combination is unique and cannot be considered as the additive contribution of each environmental factor [83–85].

Most studies of temperature acclimation did not control air humidity, which raised VPD and might flaw the effect of temperature due to the high sensitivity of transpiration to increasing VPD [41,86,87]. Moreover, the transpiration response to VPD was shown to acclimate with the prevailing VPD during growth [88–90]. Therefore, comparing results of temperature acclimation from studies conducted at different VPD may be controversial [91]. In the other hand, the direct response of gas exchange to temperature, by adjusting ambient humidity to maintain the same VPD, has been examined far less extensively [92]. Therefore, disentangling the direct effect of warming from the soil and the atmospheric drought (e.g. soil water deficit and high air VPD) requires further studies because shifts in resource allocation, morphological and physiological acclimation to warming can increase the vulnerability to overcome droughts [12,51].

In the present study we exposed one-year-old seedlings of *Fagus sylvatica* L. grown under optimal (25 °C) and supraoptimal (+7.5 °C) temperatures, to a cross-combination of water deficit and shade. VPD was kept constant at the two growing temperatures, with the aim to evaluate how warming affects the potential mechanisms that confer multi-tolerance to drought and shade [85]. We hypothesized that: 1) Warmer temperatures will reduce plant growth due to reduced leaf area rather than by a proportional decrease in photosynthesis rate, which will exacerbate the detrimental effects of combined water deficit and shade. 2) Stomatal conductance is expected to increase under warming when water is not limiting to foster evaporative cooling of the leaves, but it will be decreased when combined with water deficit. 3) The xylem anatomical traits associated with the plant hydraulic conductivity will adjust accordingly with the changes in leaf transpiration to coordinate water demand and supply. 4) Phenotypic plasticity to water availability and light intensity will be reduced due to warming.

 doi:10.20944/preprints202504.1808.v1

2. Results

Changes in Morphology and Biomass Allocation

Warming had a significant effect in plant growth and biomass after 90 days from the beginning of the experiment (Table 2). Plants in T25 grew thicker and produced more biomass and bigger leaves, resulting in higher leaf area. Plants in T32 produced more leaves but were smaller (Figure 1; Table A1). Plant growth was closely related with leaf net photosynthesis (An) across treatments (Figure 1). Both water deficit and low light conditions reduced growth, biomass and the number of fully developed leaves, although the cumulative effect of light intensity exerted a stronger effect than water deficit (Figure 1). Water deficit increased the water use efficiency of leaves (Figure 1). Plants grew in low light produced the least biomass at both growth temperatures and water treatments. Growth temperature changed the biomass allocation pattern and plants in T32 allocated more resources to leaves and less to shoots than in T25, and water deficit increased the proportion of root biomass (Table 2; Figure A2).

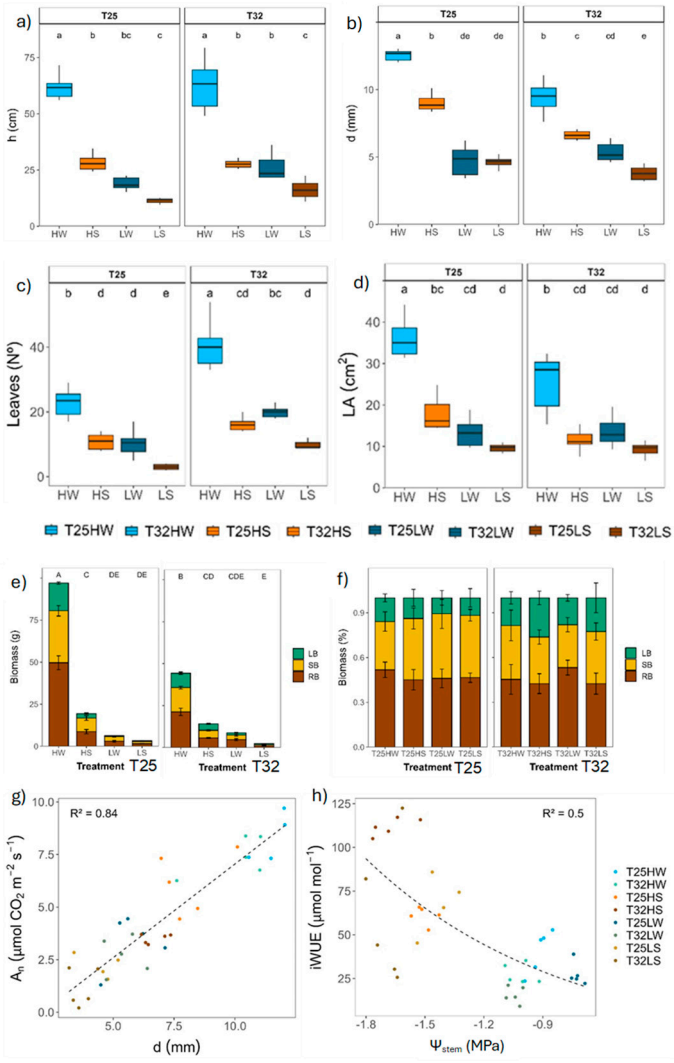

Figure 1. Plasticity of growth and biomass allocation of beech seedlings growing at 25 °C (T25) and 32 °C (T32) and two water and light treatments: **a**) height (h); **b**) diameter (d); **c**) number of developed leaves; **d**) mean leaf area (LA); **e)** total biomass of leaves (LB), shoots (SB), and roots (RB) and **f**) relative proportion of biomass (%) for leaves (LB), shoots (SB), and roots (RB). Each bar or box plot represent (mean ± SE). HW (high light well-watered), HS (high light water-stressed), LW (low light well-watered), LS (low light water-stressed). Each boxplot represents the interquartile range (IQR), with the lower and upper edges corresponding to the first (Q1)

 doi:10.20944/preprints202504.1808.v1

and third (Q3) quartiles, respectively. The straight horizontal black line within each box indicates the median Different letters indicate significant differences among treatments. **g**) strait line regression between net photosynthesis (A_n) and stem diameter (d) and **h**) second order polynomial regression between intrinsic water use efficiency (*iWUE*) and stem water potential at midday (Ψ_{stem}).

Table 2. F-statistics from a full-factorial mixed effect ANOVA using growing temperature (Tgrowth), watering (Water) and light intensity (Light) as fixed effects with n = 5 replicates as random effect. Significant outcomes are indicated in bold with P-values < 0.05 indicated as ∗, P < 0.01 as ∗∗ and P < 0.001 as ∗∗∗ in the table. The factor or combination of growing factors with highest F score for each variable were marked in grey. Same abbreviations for variables than in Table 1.

Variables	Tgrowth	Light	Water	Tgrowth x Light	Tgrowth x Water	Light x Water	Tgrowth x Light x Water
h	**6.70 ***	**297.50 *****	**193.51 *****	3.16	0.76	**67.01 *****	<0.01
d	**42.33 *****	**520.49 *****	**98.20 *****	**42.15 *****	1.05	**29.80 *****	**6.72 ***
Leaves	**100.86 *****	**145.62 *****	**188.08 *****	**7.40 ****	**23.78 *****	**34.68 *****	2.88
TLA	**9.40 ****	**300.24 *****	**276.75 *****	**39.46 *****	**45.09 *****	**150.84 *****	**60.06 *****
LA	**14.39 *****	**89.00 *****	**74.64 *****	**12.26 ****	0.89	**26.41 *****	1.16
RB (abs)	**41.51 *****	**240.44 *****	**149.30 *****	**45.23 *****	**24.45 *****	**109.47 *****	**35.29 *****
SB (abs)	**19.35 *****	**145.18 *****	**74.65 *****	**15.00 *****	**5.46 ***	**55.17 *****	**6.45 ***
LB (abs)	**8.48 ****	**267.33 *****	**122.04 *****	**15.91 *****	**18.65 *****	**90.60 *****	**27.50 *****
RB (rel)	0.30	0.71	**9.25 ****	**4.69 ***	**5.96 ***	0.02	**5.29 ***
SB (rel)	**15.35 *****	**4.59 ***	1.84	3.93	0.03	<0.01	**4.80 ***
LB (rel)	**25.41*****	1.53	2.84	1.08	**4.37 ***	<0.01	1.17
A_n	**18.99 *****	**169.38 *****	**52.01 *****	2.37	2.77	**7.88 ****	0.95
R_l	**195.44 *****	**66.12 *****	**229.84 *****	3.53	0.19	**67.24 *****	**10.88 ****
g_{sw}	0.01	**26.59 *****	**119.13 *****	1.21	**9.21 ****	**4.94 ***	0.70
g_{min}	**652.60 *****	**700.90 *****	**1149.90 *****	**232.70 *****	**379.90 *****	**470.70 *****	**432.10 *****
E	0.15	**50.60 *****	**195.30 *****	2.74	**26.13 *****	2.79	2.03
iWUE	1.02	**108.38 *****	**390.07 *****	**77.93 *****	**17.56 *****	**18.80 *****	**84.06 *****
WUE	**7.26 ***	**59.41 *****	**97.25 *****	**38.82 *****	2.68	**6.81 ***	**44.05 *****
LMA	**264.22 *****	**505.64 *****	**166.07 *****	**22.42 *****	**111.74 *****	**7.13 ****	**118.75 *****
$\delta^{13}C$	**31.65 *****	**50.34 *****	**11.99 ****	0.08	0.37	0.13	0.32
SD	0.59	**10.49 ****	0.29	**4.55 ***	0.77	0.62	0.82
LS	<0.01	2.98	**11.35 ****	0.67	**6.55 ***	0.33	0.22
PCI	1.00	**27.23 *****	**6.87 ***	**7.18 ***	**11.39 ****	0.03	2.03
C_Π^0	1.49	**5.69 ***	**21.60 *****	1.00	**5.47 ***	3.01	0.22
C_ Π^{100}	**33.79 *****	**22.46 *****	**86.54 *****	0.49	**14.93 *****	**22.86 *****	0.33
Π^0	**5.02 ***	1.43	2.46	0.11	**11.08 ****	**6.28 ***	1.67
Π^{100}	0.27	**4.25 ***	**16.44 *****	1.40	**16.27 *****	**4.50 ***	0.88
ε_{leaf}	0.28	0.04	**9.40 ****	0.11	**7.08 ***	**4.19 ***	0.66
Ψ_{leaf}	**69.36 *****	**29.73 *****	**737.58 *****	**6.85 ***	0.01	<0.01	**4.305 ***
Ψ_{stem}	**59.97 *****	**15.49 *****	**710.44 *****	**12.86 ****	0.07	0.35	0.75
Ψ_{pd}	**46.04 *****	**11.67 ****	**852.71 *****	1.87	0.03	3.55	4.87 *
SM_{leaf}	**13.28 *****	3.69	**107.36 *****	0.41	**5.42 ***	**5.53 ***	**29.57 *****
Ks	0.14	**32.26 *****	**28.46 *****	0.38	0.81	0.01	0.93
Kl	**90.41 *****	0.40	**221.90 *****	0.85	**74.61 *****	**27.33 *****	**54.54 *****
Hv	**76.66 *****	**15.01 *****	**99.57 *****	1.45	**55.79 *****	1.05	**6.37 ***
k_{plant}	0.39	**23.98 *****	**256.35 *****	0.01	**7.94 ****	2.54	3.85
VD	**48.24 *****	**447.68 *****	**2158.38 *****	**55.35 *****	**42.96 *****	**5.88 ***	**87.85 *****

 doi:10.20944/preprints202504.1808.v1

VA	**261.49 *****	**893.15 *****	**2680.29 *****	**90.51 *****	**90.14 *****	**111.22 *****	**148.31 *****
RP	2.17	0.05	0.93	3.67	3.00	0.06	<0.01
Dh	**245.32 *****	**1165.82 *****	**3405.51 *****	**11.11 ****	**52.28 *****	**14.03 *****	**190.31 *****

Leaf Gas Exchange, Water Use Efficiency and Stomatal Traits

Leaf gas exchange was significantly affected by temperature, light intensity and watering during growth (Table 2). Unlike for net assimilation (A_n), for which light intensity exerted the stronger effect, water treatment was the main regulator of g_{sw}, R_l, g_{min} and *iWUE*, particularly in T32 (Table 2). Nevertheless, warming significantly decreased A_n and increased R_l, but g_{sw} and g_{min} increased only under well-watered conditions (Table 2), thereby decreasing *iWUE*, which aligns with more negative isotopic carbon composition of leaves grew at both light conditions ($\delta^{13}C$) (Figure 2). Warming when combined with water deficit had a more negative effect on leaf gas exchange for any light growth condition. Stomatal traits were not directly affected by warming although warming had significant interaction with the other two growing factors. Stomatal density (S_D) was mostly affected by the light intensity (higher at higher intensity) only at T25, but stomatal length (L_s) was mostly affected by available water (shorter stomata under water deficit) only at T32.

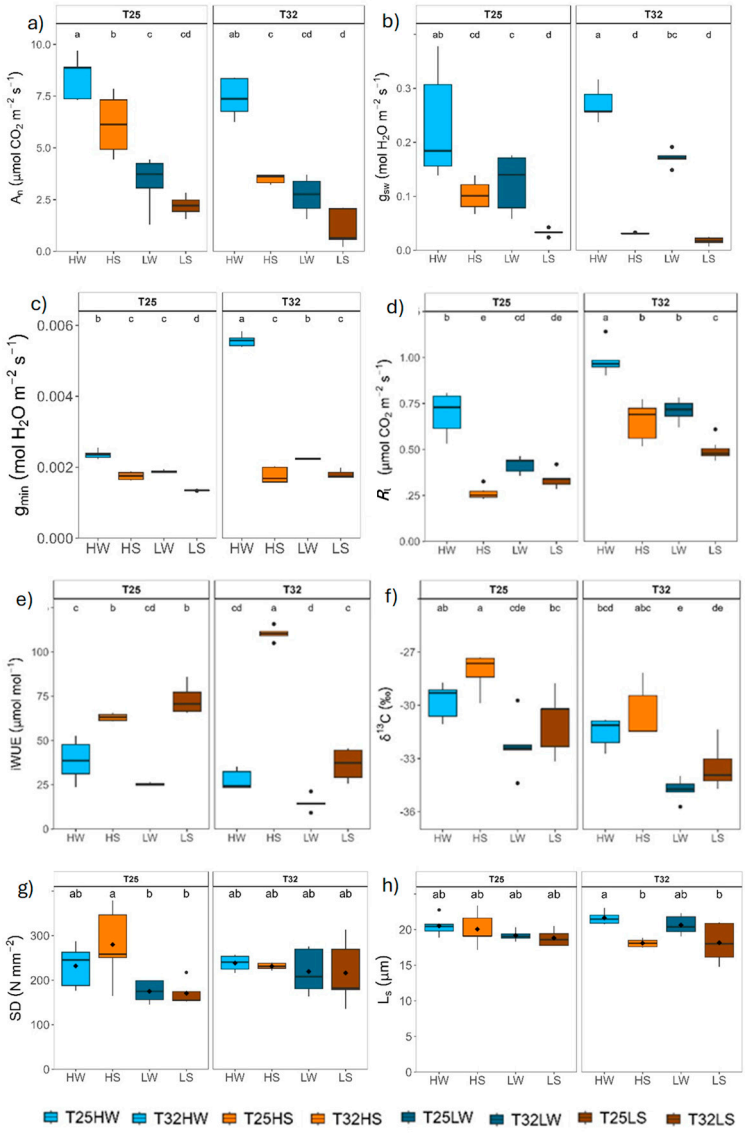

Figure 2. Plasticity of leaf gas exchange, isotopic carbon composition and stomatal traits: **a**) net assimilation (A_n); **b**) stomatal conductance to water vapor (g_{sw}); **c**) minimal conductance (g_{min}); **d**) mitochondrial respiration in the

 doi:10.20944/preprints202504.1808.v1

light (R_l); **e**) intrinsic water use efficiency (iWUE); **f**) carbon isotope composition ($\delta^{13}C$); **g**) stomatal density (SD) and **h**) stomatal length (L_s) under different treatments: HW (high light well-watered), HS (high light water-stressed), LW (low light well-watered), LS (low light water-stressed) and growth temperatures (T25, T32). Each boxplot represents the interquartile range (IQR), with the lower and upper edges corresponding to the first (Q1) and third (Q3) quartiles, respectively. The straight horizontal black line within each box indicates the median Different letters indicate significant differences among treatments.

Leaf Water Relations

Water availability was the main factor affecting leaf water relations, although warming lowered leaf water potentials (Ψ_{pd}, Ψ_{leaf} and Ψ_{stem}) in T32 more than in T25. Growing at high light produced significant more negative leaf water potentials (Figure 3; Table 2). Most parameters derived from the P-V curves were significantly affected by water availability, although with strong interactions with light and temperature. In T25, well-watered plants showed higher osmotic potential at full turgor and loss of turgor (π^{100}, π^0) than under water deficit, 0.8 MPa of osmotic adjustment at high light intensity, and higher leaf capacitance before the turgor loss point (C_π^{100} or C_{FT}) but lower maximum modulus of elasticity (ε_{leaf}) than under water deficit at both high and low light intensity. However, warming prevented the capacity of osmotic adjustment of plants growing under high light intensity and reduced the plasticity to light and water in T32. By contrast, warming reduced the safety margin (SM_{leaf}, i.e. the difference between the minimum leaf water potential at midday and the potential at turgor loss point) in T32 in all treatments, particularly lower under water deficit treatments.

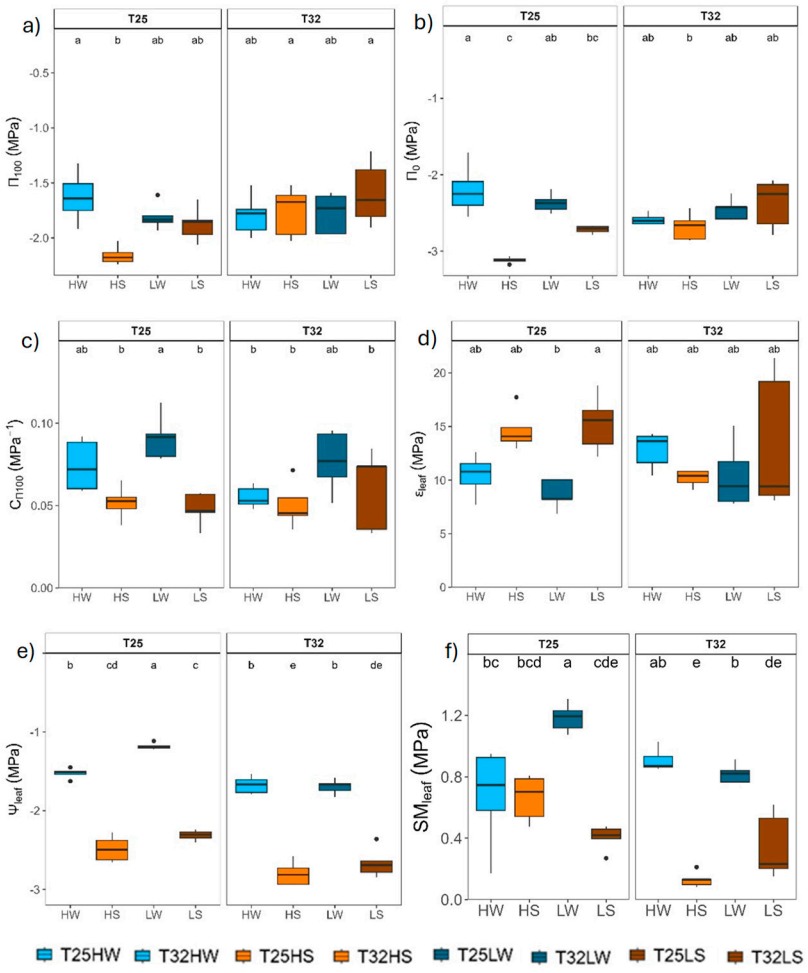

Figure 3. Plasticity of leaf water relationships: **a**) osmotic potential at full turgor (π^{100}); **b**) osmotic potential at turgor loss point (π^0); *c)* leaf capacitance before the turgor loss point ($C_{\pi 100}$); **d**) maximum modulus of elasticity (ε_{leaf}); **e**) leaf midday water potential (Ψ_{leaf}) and **f**) safety margin (SM_{leaf}) under different treatments: HW (high

 doi:10.20944/preprints202504.1808.v1

light well-watered), HS (high light water-stressed), LW (low light well-watered), LS (low light water-stressed) and growth temperatures (T25, T32). Each boxplot represents the interquartile range (IQR), with the lower and upper edges corresponding to the first (Q1) and third (Q3) quartiles, respectively. The straight horizontal black line within each box indicates the median Different letters indicate significant differences among treatments.

Hydraulic Traits and Stem Anatomy

All functional traits related with water flow were severely affected by water deficit, as expected, although the stem specific hydraulic conductivity (K_s) was more affected by light intensity than for water availability (Table 2), resembling what was observed for morphological traits (e.g. plant height, diameter and total leaf area). Warming did not have a significant effect on K_s and only a moderate increase on the plant hydraulic conductance (k_{plant}) under high light and well-watered conditions (Figure 4). In contrast, warming decreased the leaf specific hydraulic conductivity (K_L) and Huber value (H_v) in all treatments except for well-watered plants at high light intensity. Shade significantly decreased K_s at T25 and increased H_v and K_l in T25 well-watered plants, but not in T32, and decreased k_{plant} only at T32. The mean loss of xylem conductivity (PLC) was lower than 10% in well-watered plants and lower than 16% in water-stressed pointed to moderate drought during the whole experiment.

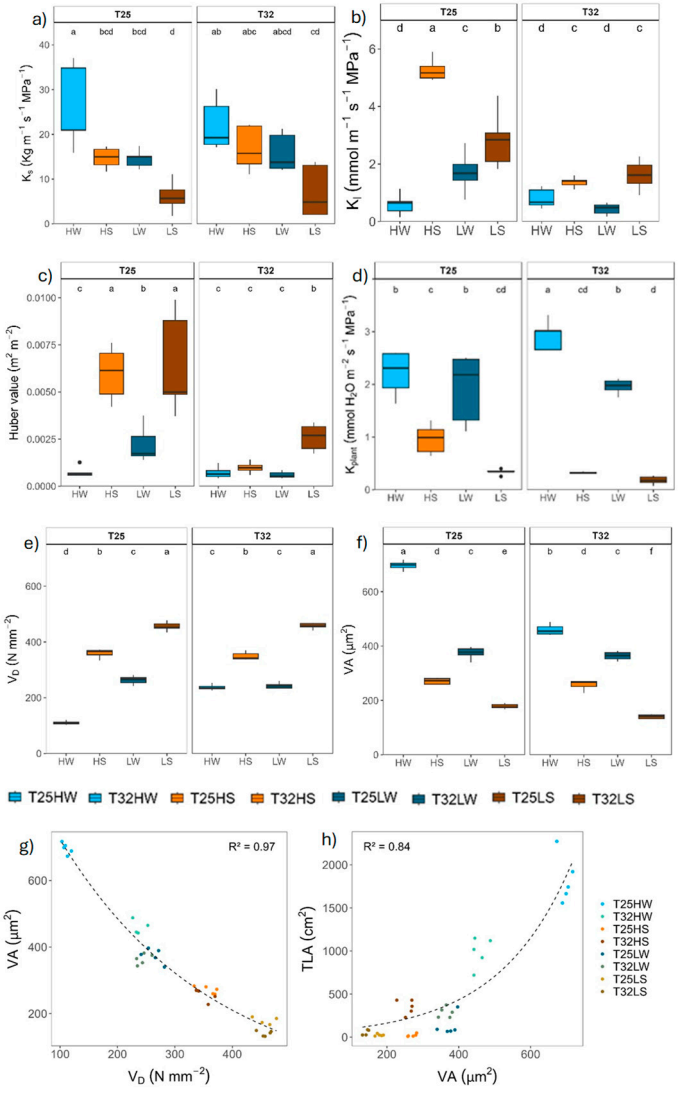

Figure 4. Plasticity in hydraulic traits and stem anatomy: **a**) stem specific hydraulic conductivity (K_s); **b**) leaf specific hydraulic conductivity (K_{leaf}); **c**) Huver value (H_v); **d**) plant hydraulic conductance (k_{plant}); **e**) vessel

 doi:10.20944/preprints202504.1808.v1

density (V_D) and **f**) average vessel area (V_A) under different treatments: HW (high light well-watered), HS (high light water-stressed), LW (low light well-watered), LS (low light water-stressed) and growth temperatures (T25, T32). Each boxplot represents the interquartile range (IQR), with the lower and upper edges corresponding to the first (Q1) and third (Q3) quartiles, respectively. The straight horizontal black line within each box indicates the median. Different letters indicate significant differences among treatments. **g**) and **h**) are strong correlations negative between V_D and V_A and positive between V_A and total plant leaf area (TLA).

Stem xylem anatomy was remarkably affected by water stress, which induced an increase in vessel density by unit of xylem area (V_D) but lower vessel area (V_A) and hydraulic diameter (D_h) than under well-watered conditions. Growing at high light intensity produced higher V_A and lower V_D. Indeed, we found a strong trade-off between V_D and V_A and an exponential relationship between TLA and V_A across all treatments (Figure 4). Warming decreased V_A and increased V_D under well-watered conditions and slightly under shade and water deficit (LS). However, for the rest of the treatments, growth temperature did not affect xylem anatomy. No significant differences between treatments were observed in the xylem area occupied by radial parenchyma.

Plasticity in Response to Temperature, Light, and Water Availability

Light and water availability significantly affected *F. sylvatica* phenotypes at different organization levels. These changes were also significantly modulated by growth temperature and for many traits, growing at warmer temperatures limited their phenotypic plasticity (Figure 5). For example, the phenotypic plasticity index (PPi) in response to growing light intensity was consistently higher at T25 than at T32 under well-watered conditions, although only higher regarding leaf gas exchange when evaluated under water stress (Figure 5). PPi was also higher for water availability for most traits except for leaf gas exchange at high light intensity, because the combination of warming and water stress reduced leaf gas exchange more at T32 than at T25. Under shade, plasticity for water deficit was higher at T32 in all but for leaf water relations, and higher adjustments were observed at T25 than at T32 (Figure 5). Overall PPi for all treatments and variables is presented in Figure A6.

The degree of plasticity differed among traits. Traits related with cumulative growth were among the most plastic, including biomass partitioning (Figure 6). By contrast wood density (ϱ) showed little plasticity although significant for many treatments including an increase due to water deficit or warming (Figure 6). Stomatal morphology showed little variation and density was more plastic that stomata size. The minimum conductance to water vapour, or epidermal conductance (g_{min}), vessel density (V_D) and the number of leaves showed the highest increases in response to warming at high light whereas biomass, particularly roots, and capacitance at the turgor loss point (C_{TLP}) presented the highest reductions (Figure 6). Finally, when plants grew with low light and low water availability, a higher growth temperature resulted in decreased H_v and leaf specific conductivity (K_L) and plant hydraulic conductance (k_{plant}) (Figure 6).

Preprints.org (www.preprints.org) | NOT PEER-REVIEWED | Posted: 22 April 2025 doi:10.20944/preprints202504.1808.v1

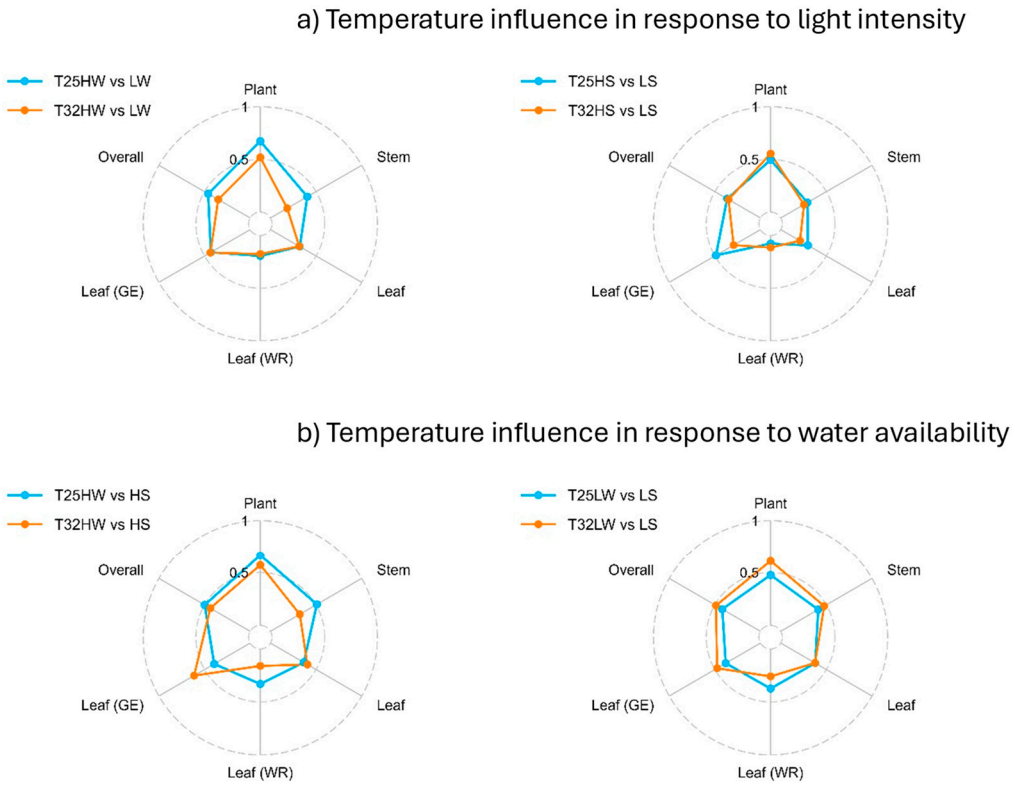

Figure 5. Radar plots of temperature influence over the Phenotypic Plasticity Index (PPi) in response to different stressors: a) light intensity and b) water availability. Traits were grouped into different organizational levels according to Table 1 into Plant, Stem, Leaf (including both Water relations + Gas exchange), Leaf (WR) (leaf water relations only), Leaf (GE) (leaf gas exchange only) and overall. Treatments area: HW (high light intensity & well-watered), HS (high light intensity & water stress), LW (shade & well-watered), LS (shade & water stress) and growth temperatures (T25, T32).

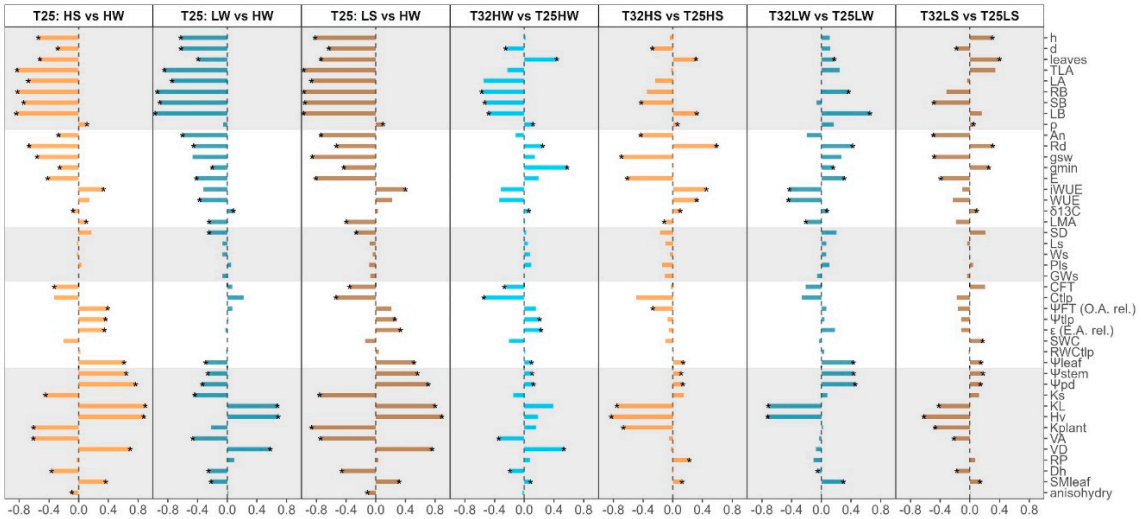

Figure 6. Relative response, or plasticity score, of each trait to each growing factor. From left to right the first three columns analyze the effect of water deficit at high light (HS vs HW), of light intensity under well-watered conditions (LW vs HW) and the combined effect of water deficit and shade (LS vs HW) at the growing temperature of T25, the next columns the effect of growing temperature under well-watered conditions and high light intensity (T32HW vs T25HW), the effect of growing temperature under water deficit conditions and high light intensity (T32HS vs T25HS), the effect of growing temperature under well-watered conditions and shade

 doi:10.20944/preprints202504.1808.v1

(T32LW vs T25LW) and finally the effect of growing temperature under water deficit and shade (T32LS vs T25LS). Negative plasticity score (NP, ranging from -1 to 0, see Material and Methods for equation) was used when the first treatment (the one on the left side of the comparison) had lower values than the reference treatment (the one on the right side) and is referred to mean values of the reference treatment.

Correlations Among Traits and Principal Components Analysis (PCA)

Plant growth traits (height and diameter) were strongly correlated among them and in general exhibited strong positive correlations with leaf gas exchange rates, K_s and V_A, irrespectively of growing temperature (Figure 7 & Figure 8). However, the temperature closest to the optimum (T25) produced significant positive correlations between plant height and ϱ and trade-offs between height and H_v, ϱ and H_V and ϱ and iWUE, which were absent at T32. In contrast, warming (T32) led to significant positive correlations of plant diameter and LMA and k_{plant}. At T25, iWUE correlated negatively with g_{sw}, ϱ, leaf C_{FT}, k_{plant}, leaf water potentials and V_D, and positively with $\delta^{13}C$, ε_{leaf}, RWC_{TLP} and H_v. But at T32 iWUE only negatively correlated with g_{sw}, k_{plant} leaf water potentials, and SM_{leaf} and positively with K_L. In T32, L_s correlated positively with LA, number of leaves, g_{sw}, g_{min}, leaf water potentials, k_{plant}, V_A and SM_{leaf}, and negatively with K_L and V_D, but at T25 there was not direct correlation with stomatal size and only with PCI and LMA, A_n and stem diameter. Leaf water relations showed higher levels of correlation with other traits (particularly with the ones related with leaf water potentials and hydraulics, but also anatomy stem anatomy and density) at T25 than at T32.

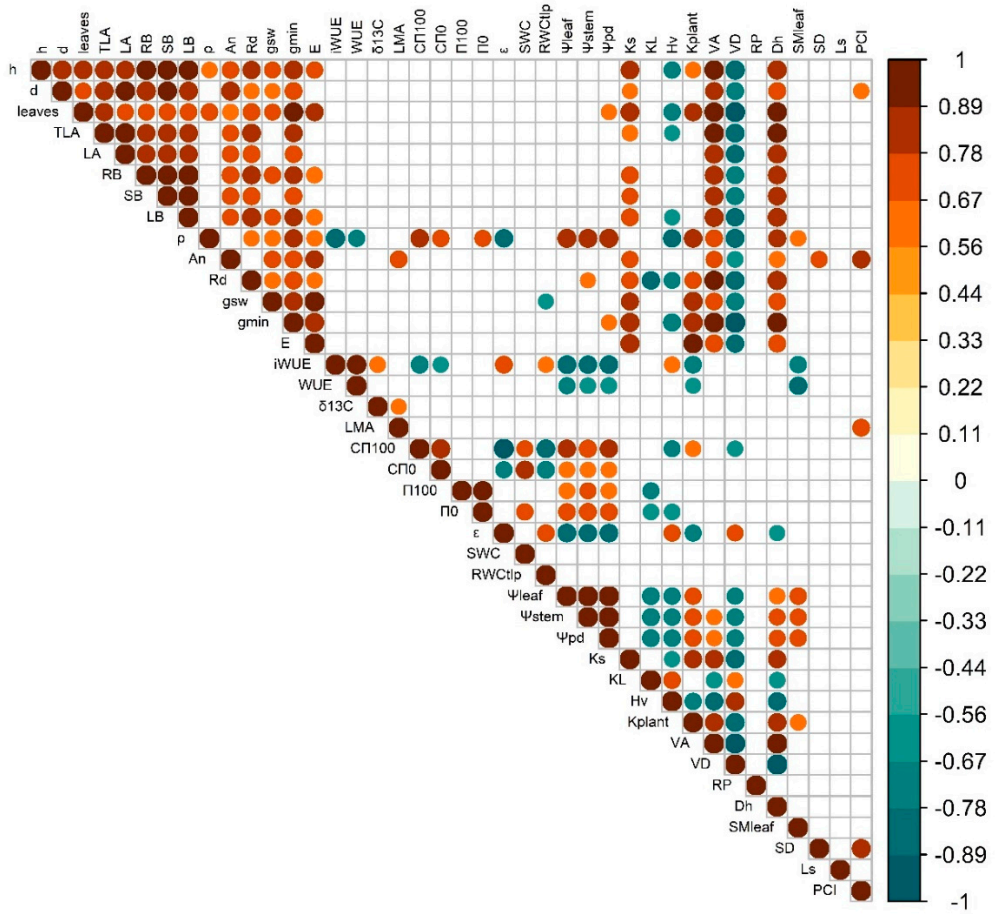

Figure 7. Pearson's correlation matrix for the evaluated traits in plants growing at T25. Significant correlations are colour coded, with positive correlations in warm colours and negative correlations in cool colours. See Table 1 for abbreviations.

 doi:10.20944/preprints202504.1808.v1

PCA was useful to characterize the two main drivers of variation: water (PC1) and light available (PC2) dividing the space into four well-characterized quadrants in clockwise order: HW, LW, LS and HS (Figure 9). The first component of PCA (PC1) explained 44 % of the variation and was positively associated with well-watered plants characterized by high values of k_{plant}, V_A, E, Ψ_{pd}, Ψ_{leaf}, and TLA; and negative scores were associated with water stressed plants for traits related with WUE, V_D, K_L and ε_{max}. PC2 explained 22 % of variation and was positively related with light intensity through LMA, $\delta^{13}C$, A_n, and S_D and negatively with SWC, π_0 and $C_{\pi 100}$. Growing temperature pushed T25 plants towards more positive score of PC1 when well-watered, but less negative PC1 and more positive PC2 under water stress and high light and less negative PC2 under shade and water stress (Figure 9).

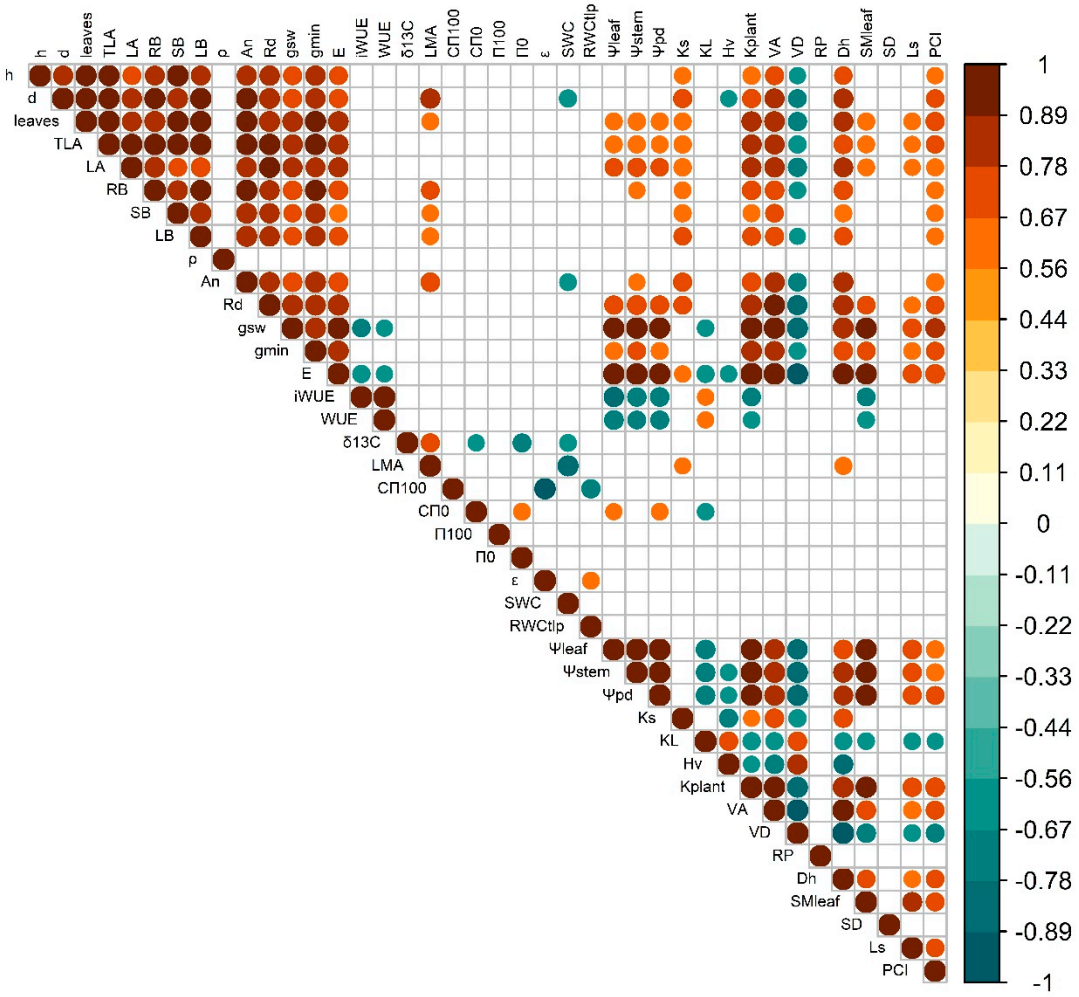

Figure 8. Pearson's correlation matrix for the evaluated traits in plants growing at T32. Significant correlations are colour coded, with positive correlations in warm colours and negative correlations in cool colours. See Table 1 for abbreviations.

 doi:10.20944/preprints202504.1808.v1

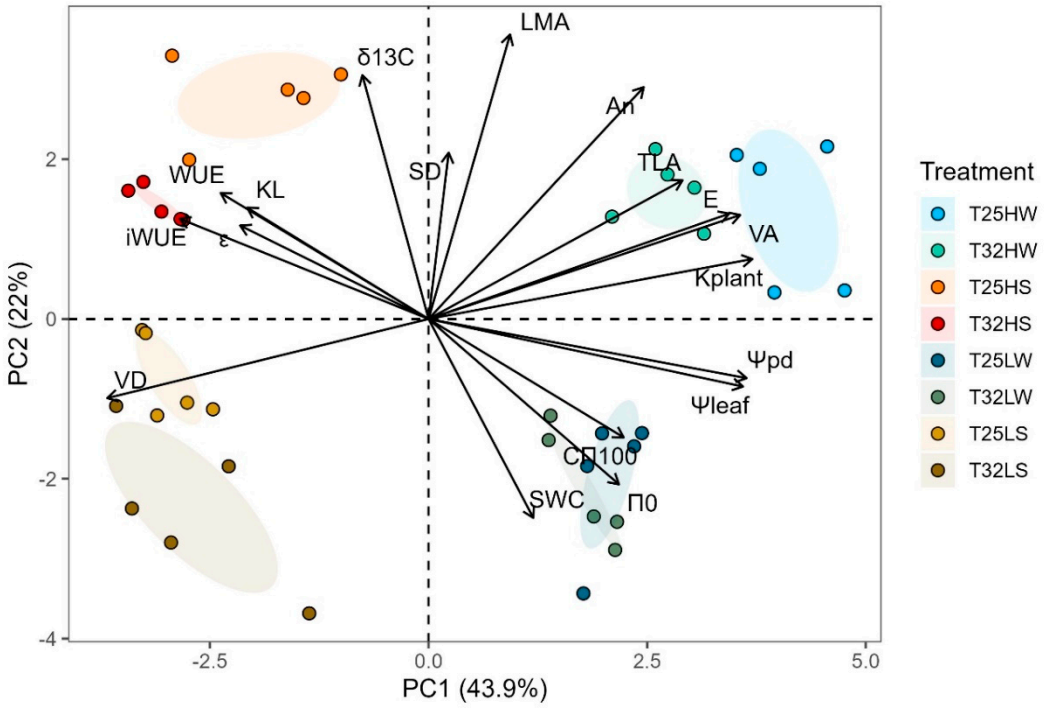

Figure 9. Principal Component Analysis (PCA) for the evaluated traits. Arrows represent the eigenvectors of each variable for the first two principal components (PC1 and PC2). The direction and length of the arrows indicate the contribution and importance of each variable to the principal components. Each plant is represented by a different colour depending on the treatment. The oval areas represent the centroids of each treatment ± 75 % of the variation within the treatment.

3. Discussion

Temperature is one of the most important determinants of plant function and development, although we know little about how temperature directly affects tree performance and physiology compare with other stresses such as drought or shade. The present study is among the first to disentangle the effect of growth temperature after controlling vapor pressure deficit (VPD) on key morphological, physiological, and anatomical traits in forest tree seedlings. Furthermore, we full fill a gap of knowledge by addressing the effect of warming in combination with superimposed stressors such as water deficit and shade in tree species, what was recently termed "multifactorial stress combination" and studied mostly in model plant species [93,94]. We revealed that warming exerted a direct influence on many of the functional traits related to plant growth and physiology (mostly negative; Figure 6), phenotypic plasticity to shade (positive) or water deficit (highly negative) and that some specific adjustments commonly observed at temperatures close to the optimum (e.g. T25) were absent when seedling were growing at supraoptimal temperatures (i.e. T32). Nevertheless, *F. sylvatica* seedlings showed strategies towards a better acclimation to warming that arguably may have improved plant performance. We discussed the extent of plant acclimation to warming and how warming may have affected the shade and drought tolerance of this late successional species.

Impact of Warming on Plant Morphology, Physiology and Anatomy at High and Low Irradiance

Warming reduced plant biomass and stem diameter (Figure 1), whereas height was less affected or even promoted under shaded conditions, which is consistent with previous studies of tree species growing near their warmer range limit [13,95,96]. Wood density (ϱ) increased at warmer temperature which could compensate for the higher height/diameter ratio of warmed plants and favor stem biomechanics [97]. Indeed, the increase in ϱ was associated with higher V_D and lower V_A in warmed

 doi:10.20944/preprints202504.1808.v1

plants growing at high irradiance (Figure 4), hence increasing the wood volume occupied by cell walls. Denser wood, associated with lower hydraulic diameter, can limit hydraulic conductivity and efficiency of water transport, although it can be an advantage in case of xylem embolism [98,99]. In fact, a strong positive correlation was found between V_A and K_s, but negative with V_D, which is indicative of the trade-off between mechanical and hydraulic efficiency. Nevertheless, despite the reduction in V_A in response to growth temperature, K_s could be partially compensated for the decrease in viscosity of water as temperature increased [100,101]. Well-watered seedlings of trembling aspen reduced leaf hydraulic conductance by 30 % as consequence of +5 ºC warming, although kept stem K_s similar across treatments (Figure 4) [41]. Our results highlight the acclimation capacity to warming of xylem conductive elements of beech seedlings confirming our third hypothesis, in contrast to the limited xylem responses of gymnosperms exposed to prolonged experimental warming [40].

Warmed plants at high irradiance (T32 HW) also produced lower leaf area (*TLA*) than plants at T25. However, under shaded conditions (LW) T32 plants produced higher *TLA* and more leaves with lower *LMA* (Figure A3). Although leaf area was positively associated with growing temperature in natural beech forest of Central Europe [57,102], an excess of warming may induce a significant reduction in leaf thickness, cell size, and total leaf area, alongside decreased starch content under high irradiance [103]. Here, the reduction of *TLA* at high irradiance was due to reduced leaf size, despite the number of leaves increased. Smaller leaves can cooldown more easily by evaporative cooling due to lower resistance of the boundary layer [22,57,104]. The same pattern was observed in warm-adapted *Populus* trees, which down-regulated leaf temperature by producing smaller and thinner leaves with higher stomatal density [105]. Hence, warming promoted a conservative production of transpiring tissue under high irradiance despite VPD was kept equal among temperature treatments, which correlated with a concomitant decrease in V_A indicating a close correlation between transpiration rate at the plant level and water supply [106–108].

Biomass of T32 HW plants was reduced by half compared to T25 HW plants, which was associated with lower carbon gain capacity (TLA decreased from 1800 cm^2 at T25 to 1000 cm^2 at T32, and 15 % reduction in A_n), together with increased carbon losses (e.g. R_d was 25 % higher at T32), confirming partially our first hypothesis (Figures 2 and A2). The temperature optimum for A_n in beech was estimated at 24.5 °C [109], hence the little reduction of A_n at 32 °C could be attributed to thermal acclimation, maybe by rising A_n optimum temperature at T32 [12,26]. In any case, the depletion of A_n might be associated with metabolic constraints, particularly the downregulation of leaf photochemistry, which frequently occurs under elevated temperatures [110,111], than to diffusional limitations to CO_2 transfer by stomata. T32 HW plants increased g_{sw} (+48 %) in response to warming at similar VPD, confirming previous studies of warming at constant VPD [92], and our second hypothesis. Other studies combining warming with elevated VPD showed no changes or decrease in g_{sw}, although the transpiration rate (*E*) increased significantly (Figure 2) [33,111,112]. Even though we ensure a similar growing air VPD, the leaf to air VPD should be slightly higher for plants growing at T32, and thus *E* was slightly higher at T32, because leaf temperature and the saturated water vapor partial pressure within the leaf was higher at T32. The rise in g_{sw} and *E* experienced by T32 HW plants correlated also with higher k_{plant} suggesting strong coordination between water supply and demand at the plant level. Higher temperatures also promoted faster water use which eventually leads to faster depletion of soil water for warmed plants [113]. Reduction in *TLA* at T32 HW was important to avoid lowering Ψ_{leaf}, beyond the leaf safety margin (SM_{leaf}) since Ψ_{tlp} did not change with temperature. Reduced *LMA* was evident in T32 HW to regulate leaf temperature and reduce leaf construction costs [114], although the lower *LMA* precluded lower leaf capacitance either before or after turgor loss than in T25 HW leaves (Figure 6), partially supporting previous studies [41].

Plasticity of g_{min} to warming or shade remains largely unexplored [61,115]. g_{min} doubled at T32HW and was significantly higher at T32LW than at T25LW (Figure 2), confirming that g_{min} is strongly dependent on temperature (Table 2) [33,61,116] found for beech that both high VPD and high temperature reduced g_{min} in the absence of soil drought, whereas our results pointed to an

 doi:10.20944/preprints202504.1808.v1

opposite direction, in line with [29,60]. g_{min} accounts for how easily the water vapor exits the leaf once stomata are closed. However, incomplete closure of stomata may contribute to g_{min}, along with higher permeability of cuticle + epidermis [117]. At moderate high temperature (<40 °C) the stomatal component of g_{min} is of greater importance than at higher air temperature and VPD, where the cuticle component is governing g_{min} [118]. Accordingly, we found strong correlations between g_{min} and stomatal traits, especially PCI, which suggested a lack of complete closure of the stomata as the main cause explaining the rise in g_{min} at T32.

Growing under shaded conditions, when water was not limited (LW), mitigated the negative effects of warming described above and stimulated plant growth and biomass. Indeed, T32 LW seedlings produced higher: biomass (particularly leaves and roots), number of leaves, and slightly higher wood density, stem height and diameter, in contrast to what was observed at high light intensity. Warming induced a divergent ecological strategy in well-watered beech seedlings under low light levels [69] aimed to compensate for the reduced carbon gain by unit of leaf area (lower A_n, but higher R_l) with increased *TLA*, greater allocation of biomass to leaves, higher number of cheaper leaves (lower *LMA*), lower iWUE and $\delta^{13}C$, and reduced H_V and K_L, but higher transpiration rate to increase C_i and reduce leaf temperature (Figures 2 and 4), in a way to minimize photorespiration losses [34]. As warming accelerated cell division, the total number of leaves increased [119]. At least for this late successional and highly shade-tolerant species, shade was beneficial to offset the negative effects of increased temperatures [120]. Beech seedlings growing under shade and warming followed an acquisitive strategy, prioritizing the consumption of water to cool down the leaves and mitigating leaf warming, but stimulating leaf growth with lower H_V and K_L to compensate for the reduced A_n [121,122]. T25 LW followed a more conservative strategy, with lower *TLA* and gas exchange, but higher Ψ_{leaf} and tougher leaves (high *LDMC* and *LMA*). This fast growing strategy of T32 LW could be risky if water is limited, since higher leaf area, but reduced leaf capacitance and Ψ_{leaf} lowered the leaf safety margin (SM_{leaf}) (Figure 3), which make beech shaded phenotypes more vulnerable to water stress under warming [123].

Impact of Warming and Water Deficit at High and Low Light Intensity

The hydraulic architecture (e.g. lower K_L, H_v and k_{plant}), significantly lower A_n, but higher carbon losses related to respiration and changes in morphological traits such as lower *LA*, *TLA* and *LMA* were related to lower biomass production, limited leaf osmotic adjustment and lower safety margin for plants growing under water-stress and warming (Figure 6), indicating important interactions between carbon investment and hydraulics [102,124,125]. Shade aggravated the negative effects of combined water stress and warming [69]. The impact of the concurrently multiple stress condition (i.e. water deficit, shade and warming) on beech seedlings conferred stronger pressure on plant's performance than any of the stress factors individually or in combination in line with previous studies with model plants [93,94]. This negative outcome can be viewed as the result of the trade-offs emerging to mitigate the combined effect of the two limited resources (i.e. soil water content and light intensity) amplified by the effect of warming (i.e. a state variable which constitutes a non-resource factor of stress) which exacerbated the already resource-limited stresses [126–128].

As water availability diminishes, elevated growth temperatures lead to a steeper reduction in A_n, primarily influenced by increased stomatal closure to avoid hydraulic dysfunction, but at the cost of decreased carbon uptake and growth [55]. Thus, to avoid excessive tension in the xylem and the risk of embolism, stomatal conductance decreased [129] and hydraulic resistance increased (lower k_{plant}) limiting water transfer (Figures 2 and 4) [130]. Water-stressed plants showed lower K_s but a more redundant xylem, which can be an advantage in case of xylem embolism [99]. The start of embolism formation (P12) in *Fagus sylvatica* was estimated at Ψ_{stem} below -1.8 MPa [131,132], although beech seedlings from the same population and acclimated to water deficit reached P12 at much lower levels (-2.4 MPa), suggesting very narrow xylem safety margin to preserve xylem functioning under drought [132]. Lower Ψ_{stem} and Ψ_{leaf} in droughted T32 plants may be the consequence not only of higher biomass allocation to leaves and decreased water viscosity [133] but also of lack of leaf osmotic

 doi:10.20944/preprints202504.1808.v1

and elastic adjustments. T32 HS leaves did not adjust osmotically (i.e. not change of water potential at full turgor) that together with the lower Ψ_{leaf} decreased significantly SM_{leaf} to almost 0.2 MPa. Lack of thermal acclimation was also observed for leaf capacitance and ε_{max}, decreasing further the plant's ability to tolerate fluctuations in Ψ_{leaf} and maintain turgor pressure (Figure 3) [134]. Maintenance of volume in chloroplasts by osmotic adjustment may preserve leaf photosynthetic capacity under drought [135] and prevent damage to chloroplasts from toxic concentrations of ions [136]. Reduced A_n in droughted T32 plants may also arise from lowered synthesis of protective enzymes, antioxidants and heat dissipation proteins, which are needed for mitigating the higher thermal and oxidative stress produced by the higher stomatal closure and limited leaf cooling capacity [78,137,138]. The capacity for osmotic or elastic adjustment was significantly hindered by light-limiting conditions and warming, which ultimately constrained the ability to maintain leaf turgor under conditions of water stress [139], reducing leaf gas exchange and growth [140].

In contrast, T25 HS plants were able to double A_n of T32 HS, achieve more than 0.8 MPa of active osmotic adjustment, lowering Ψ_{TLP} below 3 MPa (Figures 2 and 3; Table A3), and increased ε_{max}. Higher ε_{max} implied more inelastic (higher stiffness) cell walls, an adjustment that allowed leaves to rapidly change the water potential within the cells as the leaf loses water and extract water from drier soil [141,142]. T25 HS also showed higher leaf shedding, which increased H_V and the supply of water to the remaining leaves (higher K_L), lowering vessel area and producing a more redundant xylem, which may protect the hydraulic system from larger hydraulic failure (Figure 3; [59,143–145]), overall improving the whole plant water balance [146] and sustaining higher leaf gas exchange rates (Figure 2). Higher A_n in T25 HS could be the consequence of osmotically active metabolites [147,148] which not only stabilize enzymes and membranes, but also regulates the stomatal sensitivity to leaf water potential, allowing T25 HS archive 65 % higher g_{sw} than T32 HS (Figure 6) [149,150]. Both temperature treatments decreased g_{min} in response to water deficit which may offer significant advantages for the conservation of xylem function, particularly during warmer and drier conditions [33,151].

Phenotypic Plasticity and Regeneration Niche of Beech Seedlings Under Multi-Stress Factors

Phenotypic plasticity allows plants to modify their phenotype to match their current environment and it is considered beneficial when individuals can express superior phenotype in each environment compared to a fixed phenotype. However, there are limits and costs associated with plasticity [152]. Not every plant species is equally plastic for every trait, suggesting trade-offs derived from their potentially high cost of plastic responses and the complex interaction among traits, which are considered critical to their adaptive value for plant fitness [153,154]. Beech seedling showed high phenotypic plasticity (Figures 4 and 5), and as result of the long-term applied environmental factors, traits associated with whole-plant biomass demonstrated greater plasticity compared to those measured at the organ or tissue levels (Figure 5), although we detected strong synergistic effects with leaf gas exchange traits, and antagonistic relationships with the number of leaves, H_V and K_L (Figure 6). Some traits exhibited limited plasticity within the species and studied environments, such as those related with stomatal morphology, RWC_{TLP}, SWC, RP and ϱ (Figure 6, Figure A1), indicating higher costs [155]. Warming reduced overall plasticity, in agreement with our fourth hypothesis related to the cost associated with maintaining plasticity in resource-limited environments [156]. Interestingly, warming in the absence of water deficit increased the phenotypic plasticity of *F. sylvatica* seedlings growing at low light intensity (Figure 6), revealing the strong adaptation of this shade-tolerant species to grow in the humid forest understory [120,157]. Extensive phenotypic plasticity in key functional traits is often considered favorable for the persistence of populations under rapid climate change [4]. Nevertheless, the often-associated increase in VPD with temperature may further limit beech gas exchange [143,158] and growing in mixture with competing species, like oaks, which are also more drought tolerant but higher water consumers, may also compromise current regeneration potential for beech seedlings under climate change [54,159,160].

 doi:10.20944/preprints202504.1808.v1

4. Materials and Methods

Plant Material, Growth Conditions and Treatments

Beech seedlings were established from nuts collected in the Natural Reserve of 'Hayedo de Montejo' in 2021 (458,249; 4,551,615 UTM ETRS89). In February 2022, after three months at 4 °C in darkness and moist conditions, one seed per pot germinated within few days of difference in 9 L pots, filled with a mixture of peat and sand (75-25% v:v). Each pot was fertilised with a release fertiliser (Nutricote®, 16N:4.4P:8.3K, 2.5 gr L^{-1} of substrate). Pots were randomly arranged in two different walk-in growth chambers set at two different temperatures but the same air VPD. One chamber was set with day/night temperatures and relative humidity of 25/15 ± 0.5º C and relative humidity of 40/68 ± 1% (VPD of 1.91/0.86 ± 0.06 kPa) (named T25), close to the temperature optimum for photosynthesis for beech [109], and the other to 32.5/22.5 ± 0.5º C and 61/80 ± 1% (VPD of 1.91/0.86 ± 0.06 kPa) (named T32), both with a 12 h of photoperiod. +7.5 ºC is the expected increase in mean temperature during June to August for Western and Central Europe and Mediterranean region according to the scenario SSP5-8.5 for 34 models of AR6 CMIP6 (interactive-atlas.ipcc.ch) (IPCC, 2023). In each chamber, we established two treatments of light intensity: high PPFD (ca. 600 µmol photons m^{-2} s^{-1} at the canopy height) and low PPFD (ca. 200 µmol photons m^{-2} s^{-1} at the canopy height). Low PPFD (e.g. shaded conditions) was provided by grey polyethylene shade nets mounted on frames and was measured as the average of six different measurements using a quantum meter (MQ 200; Apogee Instruments Inc., Logan, UT, USA) in a horizontal position on leaves. Plants were developed under well-watered conditions for two months when seedlings with similar height and number of leaves were assigned to two contrasted watering treatments. Well-watered plants were watered daily in the morning to full capacity. Water-stressed plants were without watering until stomatal conductance reached 1/3 of well-watered plants (ranging from ca. 10 days in high PPFD to ca. 24 days in low PPFD) and then plants were watered every three days with an initial amount of 150 ml of water for plants under high PPFD and 65 ml of water for plants under low PPFD (about 1/3 of daily evapotranspiration in both cases). Once a week, plants were weighed and the volumetric soil water content (SWC) was measured by time domain reflectometry (TDR, Trase System I, Soil Moisture Equipment, USA) and watering amounts were adjusted to keep the same proportionality. At this time the final multifactorial design (two factors: water and light) was set for each growing temperature: (1) high PPFD (ca. 600 µmol photons m^{-2} s^{-1} at the canopy height) and well-watered conditions (HW); (2) high PPFD and moderate water stress (HS); (3) low PPFD (ca. 200 µmol photons m^{-2} s^{-1} at the canopy height) and well-watered conditions (LW); (4) low PPFD and moderate water stress (LS). Every week plants were randomly changed of position within each treatment. Every three weeks, plants were interchanged between chambers maintaining the specific warming treatment (i.e. same conditions, but different growing chambers).

Growth and Biomass Allocation

Growth and biomass were measured in six randomly selected plants of each treatment at the beginning of the experiment that were not sampled for any other measurement until harvest. Height, stem diameter and number of fully developed leaves were measured six times throughout the experiment (every 15 - 20 days) (see Figure A1). After 90 days growing at their specific treatments the same plants were harvested and biomass divided into roots, stems and leaves. Roots were separated from the soil by gentle washing under clean tap water. Samples were oven dried at 60 ºC for 7 days and weighed. We calculated root (*RM*), stem (*SM*) and leaf mass (*LM*) fractions as the ratio of organ dry mass to total plant dry mass. One representative fully mature leaf from the top canopy of each plant was scanned to get leaf area using ImageJ [161] and then oven dried at 70 ºC for 48 h for constant dry mass (Mettler Toledo AB 204) to determine the leaf mass per area (*LMA*) as the ratio of leaf dry mass to projected area. The total leaf area (*TLA*) of each plant was estimated from *LM* and *LMA*. The mean leaf area for each plant (*LA*) was calculated as *TLA* divided by the number of leaves.

 doi:10.20944/preprints202504.1808.v1

Gas Exchange and Water Use Efficiency

One fully mature leaf from the upper plant canopy was selected to measure the net photosynthetic rate (A_n, μmol CO_2 m^{-2} s^{-1}), stomatal conductance (g_{sw}, mol H_2O m^{-2} s^{-1}) and transpiration rate (E, mol H_2O m^{-2} s^{-1}) were measured twice during the experiment in five plants per treatment using a portable IRGA system (LI-6400XT) with the transparent chamber (6400-08 clear chamber) to record the leaf gas exchange at growing conditions. Measurements were conducted at growth conditions of air temperature (block temperature was set at 25 ºC for T25, and 32ºC for T32) and relative humidity to get a VPD close to 1.9 kPa. The reference CO_2 concentration was set at 400 μmol m^{-2} s^{-1} and flow rate of 300 μmol m^{-2} s^{-1}. After record of gas exchange at growing conditions, the light source was switched off inside the chambers and after 20 min of acclimation in the dark, dark respiration (R_d) was measured. Mitochondrial respiration in the light (R_l) was determined as 0.5 R_d. All measures of gas exchange variables were corrected with the minimum conductance (g_{min}) (see below) according to [147]. The leaf water use efficiency (WUE) was calculated as (A_n/E) and the intrinsic water use efficiency (iWUE) by (A_n/g_{sw}).

Stomatal Traits and Carbon Isotope Composition ($\delta^{13}C$)

The same leaves used for gas exchanges measurements were collected for carbon isotope composition ($\delta^{13}C$) and then for stomatal traits. Two leaf discs taken on each side of leaf blade were dried for 3 days at 65°C and analysed at the Stable Isotope Facility of the UC Davis (CA, USA). Isotope composition was measured with an elemental analyser (PDZ Europa ANCA-GSL, Sercon Ltd, Cheshire, UK) interfaced to an isotope ratio mass spectrometer (PDZ Europa 20-20; Sercon Ltd) with internal standards reaching $\delta^{13}C_{VPDB}$ standard deviation < 0.07 ‰. Leaf trichomes were removed using duct tape and three negative impressions were taken of the middle portion of the leaf avoiding main veins and using nail varnish. The impressions were attached to a microscope slide using transparent tape and imaged under a light microscope (Leica DM2500 LED) using the software Leica Application Suite X 3.7.2.22383 (Leica Microsystems GmbH, Wetzlar, Germany). Photomicrographs were analyzed using ImageJ [161]. Stomatal density (SD) was calculated as the number of stomata per unit leaf area (nº mm^{-2}) on three leaf areas of 1,15 mm^2 each using x10 magnification. Within each leaf area 10 stomata were randomly selected to measure in μm the guard cell length (SL), stomatal pore length (Pls), stomatal complex width (Ws) and guard cell width (GWs) using x40 magnification. The potential conductance index (PCI) was computed as PCI = $(GCL)^2$ SD 10^{-4} [162], as a surrogate of potential maximum stomatal conductance.

Minimum Leaf Conductance or Residual Conductance (g_{min})

At the same time of gas exchange measurements, one healthy, fully expanded leaf from the same plants was immediately stored in plastic zip bag with a moist tissue paper and kept in a portable cooler at 4 °C until they were taken to the laboratory. In the lab, leaves were stored at 4 ºC in darkness with the petiole submerged in water overnight until the next day for measurements. We estimated g_{min} through bench dehydration of the rehydrated leaves with the petioles sealed with a high-strength adhesive (Loctite, Prism 401)[163]. Briefly, leaf area was measured at the beginning of the dehydration and leaves were placed on top of a perforated rack at constant air temperature and relative humidity (ca. 25 °C and 46 %, respectively) without direct light and were repeatedly weighed with an analytical balance to determine the steady state rate of water lost by unit of leaf area once stomata were closed, i.e. epidermal transpiration (E_{min}, $\mathrm{mol\ H_2O\ m^{-2}\ s^{-1}}$). To get the epidermal minimum conductance by one side of the leaf (g_{min}, $\mathrm{mol\ H_2O\ m^{-2}\ s^{-1}}$) we followed the next approximation (g_{min} = E_{min} P/(2 VPD)), where P is the atmospheric pressure (94 kPa) and VPD is the air vapor pressure deficit (1.65 kPa), and the boundary layer conductance was assumed negligible.

 doi:10.20944/preprints202504.1808.v1

Pressure Volume Curves and Relate Traits

Leaf water relations were measured using pressure-volume (P-V) curves of leaves sampled at the end of night period on five seedlings per treatment. Leaves were rehydrated for six hours in the dark and at 4 °C with only the petiole immerse in distilled water. After that leaves were scanned to get the initial leaf area and were allowed to slowly dehydrate at constant room temperature using the free transpiration method [164,165]. Leaf water potential (Ψ_{leaf}) was measured with a pressure chamber (model 1000; PMS Instrument Co., Albany, USA) and leaf mass with a precision balance at intervals, starting with Ψ_{leaf} > -0.05 MPa and until ca. -3.5 MPa for HW and LW treatments and -6 MPa for HS and LS treatments. We checked all curves for oversaturation during the first steps of dehydration and when present was corrected as in [166,167]. Leaf dry mass was determined as described above. The osmotic potential at full turgor (π^{100} sometimes represented by Ψ_{FT}), the turgor loss point (π^{0} or Ψ_{TLP}), leaf capacitance before the turgor loss point (C_π^{100} or C_{FT}) and after (C_π^{0} or C_{TLP}), the maximum modulus of elasticity (ε_{leaf}), and the relative water content at the turgor loss point (RWC_{TLP}) were derived from the P-V curves according to [164] and [168].

Predawn and Midday Water Potentials

The same leaves used for gas exchanges measurements were used to determine midday leaf water potentials (Ψ_{leaf}) after cutting the petiole and sealed inside a plastic bag previously exhalated and stored in ice boxes, then transported to the lab and measured with a pressure chamber (PMS instrument; model 1505D) within 1–2 h of excision [169]. One adjacent leaf was previously covered and allowed to equilibrate for at least 3 h before midday, with cling wrap and aluminium foil to prevent transpiration, to determine the midday branch water potential (Ψ_{stem}) (i.e. non transpiring leaf). Leaf predawn water potential (i.e. end of the night period) (Ψ_{pd}) was measured the night before on the same plants. Safety margin (SM_{leaf}) was calculated as the absolute difference between the turgor loss point (π^{0}) and the transpiring leaf water potential at midday (Ψ_{leaf}). The degree of anisohydry was calculated as the ratio of Ψ_{leaf} to Ψ_{pd}.

Hydraulic Conductivity and Huber Value

Loss of hydraulic conductivity and maximum hydraulic conductivity were measured in nine seedlings per treatment at the end of the experiment following [170]. Plant transpiration was stopped 3 h before harvesting by switching off the lights and enclosing plants in black bags. Then pots were immersed in water and the stem was cut at the base. The entire above-ground portion was kept under water, tearing leaves away from shoots, and the plant distal end was cut to ensure xylem relaxation for 30 min [132]. The stem was then sequentially cut back underwater and 5 cm long segment above the cotyledons was connected to a XYL'EM apparatus (Bronkhorst, France) to measure hydraulic conductivity at low pressure (≤ 2 kPa) before (K_{init}) and after flushing the sample with degassed, filtered 2 mmol KCl solution at high pressure (0.2–0.3 MPa) for 20 min (K_{max}). Loss of hydraulic conductivity (PLC) was determined as:

$$PLC = 100(1 - K_{\text{init}}/K_{\text{max}}), \quad (1)$$

Maximum specific hydraulic conductivity (K_s) was calculated by dividing K_{max} by sapwood area and leaf specific conductivity (K_L) by dividing K_{max} by total supported leaf area. The Huber value (H_V) was determined as the ratio of K_L and K_s (i.e. sapwood area relative to leaf area). Finally, the hydraulic conductance of the whole plant (k_{plant}) was estimated as in [171]:

$$k_{plant} = \frac{E}{(\Psi_{pd} - \Psi_{leaf})} \quad (2)$$

Where E was the leaf transpiration rate and ($\Psi_{pd} - \Psi_{leaf}$) was assumed to be the water potential gradient from the soil to leaf (MPa), assuming full equilibration of plant and the soil at the end of the night period (i.e. $\Psi_{soil} \approx \Psi_{pd}$).

 doi:10.20944/preprints202504.1808.v1

Stem Xylem Anatomy

Five stem segments per treatment of those used for hydraulic conductivity measurements were selected for anatomical measurements. One centimetre in length was used to determine wood density (W_D) following [132]. 15 μm-thick crossed and tangential sections were cut using a sliding microtome (Leica SM 2400), stained with 0.1 % safranin and mounted for subsequent image analysis. Digital images of the thin sections were taken using a Moticam A1 camera (Motic, Hong Kong, China) attached to an Olympus BX50 light microscope. Images were analysed using ImageJ [161]. We measured three sectors per sample from the cross-section to quantify average vessel lumen area (V_A), vessel density (V_D), the equivalent circle diameter (D) and the hydraulic diameter (D_H) following [172]:

$$D = \sqrt{\frac{4V_A}{\pi}} \quad (3)$$

$$D_H = \left(\frac{\sum D^4}{N}\right)^{\frac{1}{4}} \quad (4)$$

Where V_A is the lumen conduit area, N it is the number of vessel elements. To determine the parenchyma surface area, a further three sectors per sample were taken from the tangential section.

Trait Variation and Plasticity

We calculated the effect of each treatment one by one and through the representation of the variation of each trait measured (see Table 1 with definitions) as a fraction of unity (ranging from -1 to 1), such as negative values meant a decrease in the trait as consequence of the treatment but positive meant an increase. If the trait decreases, or increases, due to the effect of the treatment and compared to the value of the treatment used as reference, we can use one of the next formulations to calculate plasticity:

If treatment mean of a variable ($\mu_{treatment}$) < reference mean ($\mu_{reference}$), the plasticity is negative:

$$NP = \frac{(\mu_{treatment} - \mu_{reference})}{\mu_{reference}} \quad (5)$$

If the mean of treatment ($\mu_{treatment}$) > the mean of reference ($\mu_{reference}$), the plasticity is positive:

$$NP = \frac{(\mu_{treatment} - \mu_{reference})}{\mu_{treatment}} \quad (6)$$

Note that we can get the individual trait response ratio as:

$$\frac{\mu_{\text{treatment}}}{\mu_{\text{reference}}} = NP + 1 \quad (7)$$

Or:

$$\frac{\mu_{\text{treatment}}}{\mu_{\text{reference}}} = \frac{1}{1 - PP} \quad (8)$$

Where NP and PP are the value of the negative or positive plasticity for the trait respectively.

The Phenotypic Plasticity Index (*PPi*) was calculated to assess the overall plasticity of *Fagus sylvatica* seedlings to different environmental conditions, evaluating the effects of growth temperature on light and water plasticity changes, as described by [173]. This form of expressing plasticity is relevant when several traits are analysed together, so we can visualize which traits are more plastic than the others. We calculated the *PPi* for each trait as the difference between the maximum and minimum mean values ($max\ \mu - min\ \mu$) divided by the maximum mean value:

$$PPi = \frac{max\ \mu - min\ \mu}{max\ \mu} \quad (9)$$

 doi:10.20944/preprints202504.1808.v1

Statistical Analyses

After checking the normality of the data, three-way analyses of variance (ANOVA) were performed in R v. 4.3.2 (R Development Core Team 2024) using 'Tgrowth', 'light' and 'water' as fixed factors. In all cases, the data met the assumptions of normality and homoscedasticity, a significance level of $P \leq 0.05$ was used and model assumptions were checked. Statistically significant differences between groups were assessed using the HSD Tukey post-hoc test in R v. 4.3.2 using the "agricolae" package. Principal Component Analysis (PCA) was performed in R version 4.3.2, utilizing the "stats" package for matrix calculations and the "factoextra" package for visualization support. The PCA was based on the correlation matrix, and the eigenvectors generated were analysed to identify variables exhibiting a strong association with specific principal components (PCs). Pearson correlation coefficients were estimated using the "rcorr" function in R. Results are presented as means ± standard error (SE).

5. Conclusions

Our findings underscore the significant impact of elevated temperature on plant growth, biomass partitioning and physiology of European beech seedlings. Specifically, we observed that warming decreased overall plant plasticity, reduced leaf size and allocated higher biomass to leaves while reduced leaf shedding and increased metabolic and water demands, suggesting that global warming could constrain the adaptive capacity of beech regeneration, especially near the drier margins of its distribution. Warming reduced biomass due to lowering total leaf area and net photosynthesis but increased respiratory costs and diminished the potential for beech seedlings to perform osmotic adjustment and decreased the leaf safety margin, which may compromise future survival of the species under dry conditions. Nevertheless, beech growth under shaded conditions may be increased due to an increase in the number of less costly leaves (lower *LMA*) which enhanced transpiration rate to cool down the leaf if warming occurs under deep soil and wet atmospheric conditions. This highlights the importance of understanding species-specific responses to multifactorial stress factors, which is essential for projecting the long-term persistence and ecological success of forest species under future warming scenarios.

Author Contributions: All authors contributed to the collection of data, FR led the analysis of data and the initial draft preparation supervised by RL and FJC. Funding was secured by FJC and RL. All authors have read and agreed to the published version of the manuscript.

Funding: Francisco Javier Cano acknowledges support by the Spanish Ministry of Science, Innovation and the EU through the competitive grants RYC2021-035064-I funded by MCIN/AEI/ 10.13039/501100011033 and "European Union NextGenerationEU/PRTR" and PID2023-147450OA-I00 funded by MICIU/AEI/ 10.13039/501100011033 and by "ERDF/EU". Faustino holds a PhD grant from Universidad Politécnica de Madrid. This research was supported by the project SYLVADAPT (PID2019-107256RB-I00; Spanish Ministry of Science and Innovation) and the project FAGUS by the Comunidad de Madrid through the call Research Grants for Young Investigators from Universidad Politécnica de Madrid.

Data Availability Statement: All data supporting reported results can be found in the main text and in appendix.

Acknowledgments: We are grateful to David Sánchez Gómez and María del Rey for their kindly assistance with growing chambers. FRP thanks to Universidad Politécnica de Madrid - Funded Research, Development and Innovation Program (specifically the funding for predoctoral contracts for the completion of doctoral degrees at UPM schools, faculties and R&D centers).

Conflicts of Interest: The authors declare no conflicts of interest.

 doi:10.20944/preprints202504.1808.v1

Abbreviations

The following abbreviations are used in this manuscript:

Table 1. List of studied traits, with abbreviations and units and the classification to calculate the Phenotypic Plasticity index (PPi).

Symbol	Level for PPi	Definition	Values units
h	Plant	Plant height	(cm)
d	Plant	Plant diameter	(mm)
leaves	Plant	Number of fully developed leaves	(nº)
TLA	Plant	Total plant leaf area	(cm^2)
LA	Leaf GE relations	Average leaf area	(cm^2)
RB	Plant	Root biomass	(g)
SB	Plant	Shoot biomass	(g)
LB	Plant	Leaf biomass	(g)
ϱ	Plant	Wood density	($g\ cm^{-3}$)
A_n	Leaf GE relations	Leaf net assimilation rate	($\mu mol\ CO_2\ m^{-2}\ s^{-1}$)
R_l	Leaf GE relations	Leaf respiration in the light	($\mu mol\ CO_2\ m^{-2}\ s^{-1}$)
g_{sw}	Leaf GE relations	Leaf stomatal conductance to water vapour	($mol\ H_2O\ m^{-2}\ s^{-1}$)
g_{min}	Leaf GE relations	Leaf minimum conductance to water vapour	($mmol\ H_2O\ m^{-2}\ s^{-1}$)
E	Leaf GE relations	Leaf transpiration	($mol\ H_2O\ m^{-2}\ s^{-1}$)
iWUE	Not used for PPi	Intrinsic water use efficiency	($\mu mol\ CO_2\ mol^{-1}\ H_2O$)
WUE	Not used for PPi	Water use efficiency	($\mu mol\ CO_2\ mol^{-1}\ H_2O$)
$\delta^{13}C$	Not used for PPi	Carbon isotope composition	(‰)
LMA	Leaf GE relations	Leaf mass per area	($g\ m^{-2}$)
S_D	Stomatal anatomy	Stomatal density	(nº stomata per mm^2)
L_s	Stomatal anatomy	Stomatal length	(µm)
PCI	Stomatal anatomy	Potential conductance index	($\mu m^2\ mm^{-2}\ 10^{-4}$)
W_s	Stomatal anatomy	Stomatal complex width	(µm)
Pl_s	Stomatal anatomy	Stomatal pore length	(µm)
GW_s	Stomatal anatomy	Guard cell width	(µm)
$C\_\Pi^{100}(C_{FT})$	Leaf water relations	Leaf capacitance at full turgor	(MPa^{-1})
C_Π^{0} (C_{TLP})	Leaf water relations	Leaf capacitance at turgor loss point	(MPa^{-1})
Π^{100} (Ψ_{FT})	Leaf water relations	Leaf osmotic potential at full turgor	(MPa)
Π^{0} (Ψ_{TLP})	Leaf water relations	Leaf turgor loss point	(MPa)
ε_{leaf}	Leaf water relations	Leaf maximum Young's modulus of elasticity	(MPa)
RWC_{TLP}	Leaf water relations	Relative water content at the turgor loss point	(%)
SWC	Leaf water relations	Leaf saturated water content	($g\ g^{-1}$)
Ψ_{leaf}	Leaf water relations	Leaf midday water potential	(MPa)
Ψ_{stem}	Leaf water relations	Stem midday water potential	(MPa)
Ψ_{pd}	Not used for PPi	Predawn water potential	(MPa)
SM_{leaf}	Not used for PPi	Leaf safety margin	(MPa)
Anisohydry	Plant	Ratio Ψ_{leaf} to Ψ_{pd}	(dimensionless)
K_S	Stem	Hydraulic specific conductivity	($kg\ m^{-1}\ s^{-1}\ Mpa^{-1}$)
K_L	Stem	Leaf hydraulic conductivity	($mmol\ m^{-1}\ s^{-1}\ Mpa^{-1}$)
H_v	Plant	Huber value	($m^2\ m^{-2}$)
k_{plant}	Plant	Plant hydraulic conductance	($mmol\ m^{-2}\ s^{-1}\ Mpa^{-1}$)
V_A	Stem	Average vessel lumen area	(μm^2)
V_D	Stem	Vessel density	(nº vessels per mm^2)
RP	Stem	Xylem area occupied by radial parenchyma	(%)
D_h	Not used for PPi	Hydraulic diameter	(µm)

 doi:10.20944/preprints202504.1808.v1

Appendix A

Table A1. Phenotypic plasticity index: (max mean – min mean)/ max mean Temperature response to light.

Group of variables	Measured variables	Well-watered		Water deficit	
		T25	T32	T25	T32
		Response to Light (HW vs LW)	Response to Light (HW vs LW)	Response to Light (HS vs LS)	Response to Light (HS vs LS)
Plant level	10	**0.67**	0.52	0.50	**0.56**
Stem	6	**0.40**	0.18	**0.29**	**0.26**
Leaf (PV + GE)	13	**0.32**	**0.32**	**0.30**	0.21
Leaf hydric relations	6	**0.19**	**0.18**	0.08	**0.11**
Leaf GE relations	7	**0.43**	**0.44**	**0.49**	0.29
Overall	29	**0.46**	0.35	**0.37**	**0.35**

Table A2. Phenotypic plasticity index: (max mean – min mean)/ max mean. Temperature response to water.

Group of variables	Measured variables	High light		Low light	
		T25	T32	T25	T32
		Response to Water (HW vs HS)	Response to Water (HW vs HS)	Response to Light (HS vs LS)	Response to Light (HS vs LS)
Full plant	10	**0.67**	0.57	Full plant	10
Stem	7	**0.51**	0.32	Stem	7
Leaf (PV + GE)	12	0.37	**0.41**	Leaf (PV + GE)	12
Leaf water relations	6	**0.33**	0.16	Leaf water relations	6
Leaf GE relations	6	0.39	**0.61**	Leaf GE relations	6
Overall	29	**0.50**	0.44	Overall	29

Table A3. Summary table of all the measured parameters, expressed as mean ± standard error. Sample size it is referred as n. Variables are described in Table 1.

Growth temperature		T25				T32			
Treatment		HW	HS	LW	LS	HW	HS	LW	LS
Sample size (n)		6	6	6	6	6	6	6	6
h	(cm)	61.9 ± 2.3	28.4 ± 1.6	18.9 ± 1.2	11.3 ± 0.5	63.1 ± 3.9	27.2 ± 0.8	26.2 ± 2.3	16.3 ± 1.6
d	(mm)	12.6 ± 0.2	9.0 ± 0.3	4.7 ± 0.5	4.6 ± 0.2	9.4 ± 0.4	6.6 ± 0.1	5.4 ± 0.3	3.8 ± 0.2
leaves	(n^0)	23 ± 2	11 ± 1	10 ± 2	3 ± 0	41 ± 3	16 ± 1	20 ± 1	10 ± 0
TLA	(cm^2)	1881.76 ± 113.43	214.56 ± 8.03	165.04 ± 54.89	31.34 ± 8.24	986.67 ± 68.17	328.22 ± 31.02	273.95 ± 26.37	86.74 ± 22.89
LA	(cm^2)	36.16 ± 2.02	17.88 ± 1.71	13.37 ± 1.48	9.62 ± 0.42	25.41 ± 2.98	11.51 ± 1.1	13.65 ± 1.37	9.28 ± 0.71
RB	(g)	30.9 ± 3.1	8 ± 1.3	2.9 ± 0.5	1.4 ± 0.1	14.5 ± 0.8	4.6 ± 0.3	2.7 ± 0.6	0.7 ± 0.1
SB	(g)	16.3 ± 0.8	2.6 ± 0.6	0.5 ± 0	0.4 ± 0.1	8.6 ± 0.7	3.9 ± 0.4	1.4 ± 0.2	0.5 ± 0.1
LB	(g)	49.7 ± 4.1	8.7 ± 1.2	3 ± 0.5	1.5 ± 0.1	21.2 ± 2.2	5.6 ± 0.3	4.7 ± 0.6	1 ± 0.2
TB	(g)	95.8 ± 6.5	19.3 ± 2.5	6.6 ± 1.1	4.1 ± 0.8	46.9 ± 2.6	14.8 ± 1	9 ± 1.3	2.5 ± 0.5
RB	(%)	32.4 ± 2.6	38.6 ± 1.9	43.2 ± 4	41.8 ± 1.6	32.7 ± 3	30.8 ± 0.8	28.7 ± 2	34.9 ± 2.2
SB	(%)	15.9 ± 1.1	13.1 ± 0.3	10.7 ± 2	11.7 ± 2.5	17.1 ± 1.1	24.7 ± 1.2	18.1 ± 0.9	22.6 ± 3.8
LB	(%)	50 ± 1.3	44.9 ± 1	43.8 ± 1.4	46.5 ± 1.3	45.3 ± 4.1	40.3 ± 2	55 ± 1	42.4 ± 2.7
K_s	(kg m^{-1} s^{-1} Mpa^{-1})	25.94 ± 4.21	14.78 ± 0.92	14.56 ± 0.91	6.11 ± 1.31	22.09 ± 2.58	16.85 ± 2.23	15.86 ± 1.93	7.19 ± 2.61
K_L	(mmol m^{-1} s^{-1} Mpa^{-1})	0.62 ± 0.11	5.26 ± 0.15	1.72 ± 0.32	2.84 ± 0.45	0.81 ± 0.12	1.37 ± 0.07	0.44 ± 0.08	1.62 ± 0.23

 doi:10.20944/preprints202504.1808.v1

K_{plant}	(mmol m^{-2} s^{-1} Mpa^{-1})	2.46 ± 0.31	0.96 ± 0.13	1.92 ± 0.29	0.34 ± 0.02	2.93 ± 0.12	0.32 ± 0.01	1.96 ± 0.06	0.18 ± 0.03
H_V	(cm^2 m^{-2})	7.6 ± 1	59.8 ± 6.4	21.9 ± 3.8	64.5 ± 12.1	7.2 ± 0.8	9.9 ± 0.9	6 ± 0.7	26 ± 3.2
LMA	(g m^{-2})	82.9 ± 1.4	90.2 ± 2.1	62.2 ± 1.4	49.6 ± 1.5	80.1 ± 1.9	43.9 ± 1.1	49.5 ± 0.7	40.5 ± 0.7
A_n	(µmol m-2 s-1)	8.4 ± 0.5	6.1 ± 0.7	3.4 ± 0.6	2.2 ± 0.2	7.4 ± 0.4	3.5 ± 0.1	2.7 ± 0.4	1.1 ± 0.4
R_l	(µmol m^{-2} s^{-1})	0.75 ± 0.02	0.25 ± 0.01	0.41 ± 0.02	0.35 ± 0.02	1.00 ± 0.04	0.61 ± 0.04	0.72 ± 0.03	0.51 ± 0.03
g_{sw}	(mmol m^{-2} s^{-1})	232.7 ± 46.7	101.9 ± 13	124.8 ± 24	33.2 ± 3	271.4 ± 14	31.3 ± 0.5	171 ± 6.8	17.2 ± 3.2
g_{min}	(mmol m^{-2} s^{-1})	2.36 ± 0.06	1.75 ± 0.05	1.88 ± 0.02	1.35 ± 0.01	5.57 ± 0.08	1.78 ± 0.1	2.24 ± 0.01	1.81 ± 0.05
E	(mol m^{-2} s^{-1})	3.2 ± 0.4	1.8 ± 0.2	1.9 ± 0.3	0.6 ± 0	3.9 ± 0.1	0.7 ± 0	2.7 ± 0.1	0.4 ± 0.1
iWUE	(µmol mol^{-1})	38.8 ± 5.3	63.1 ± 0.9	25.4 ± 0.4	73.2 ± 4.7	27.8 ± 2.6	110.4 ± 1.7	14.7 ± 1.9	36.5 ± 5
WUE	(µmol mol^{-1})	2.7 ± 0.2	3.3 ± 0.1	1.8 ± 0	4 ± 0.3	1.9 ± 0.1	5.3 ± 0.4	1.1 ± 0.2	1.5 ± 0.2
$\delta^{13}C$	(‰)	-29.8 ± 0.5	-27.6 ± 0.7	-32.3 ± 0.7	-30.9 ± 0.8	-31.5 ± 0.4	-30.4 ± 0.7	-34.8 ± 0.3	-33.5 ± 0.6

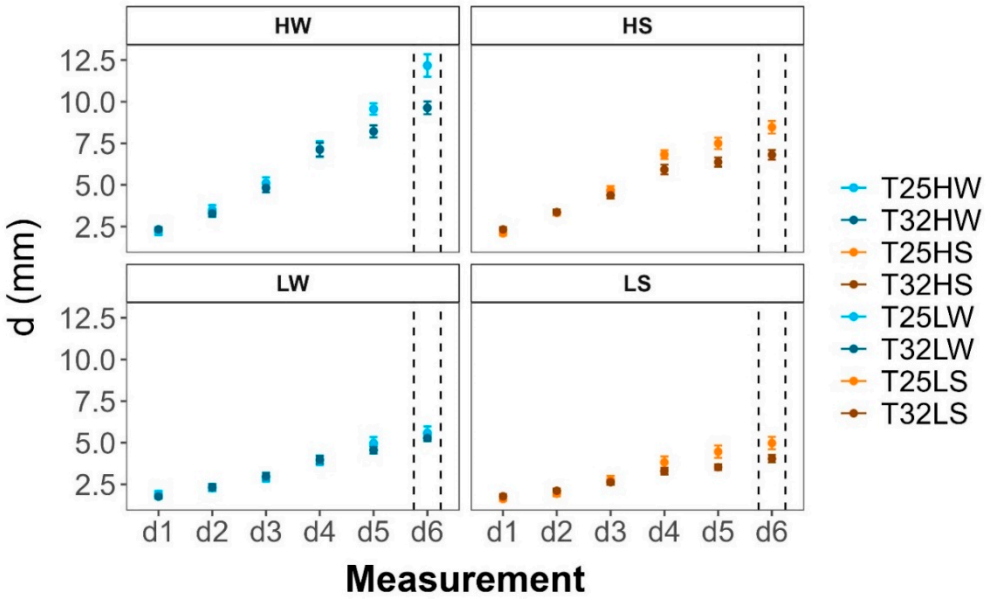

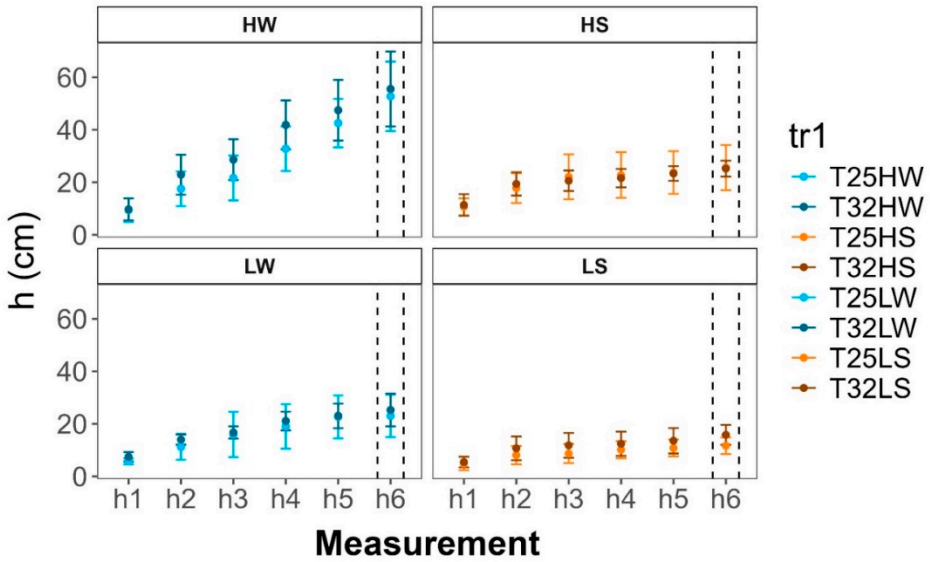

 doi:10.20944/preprints202504.1808.v1

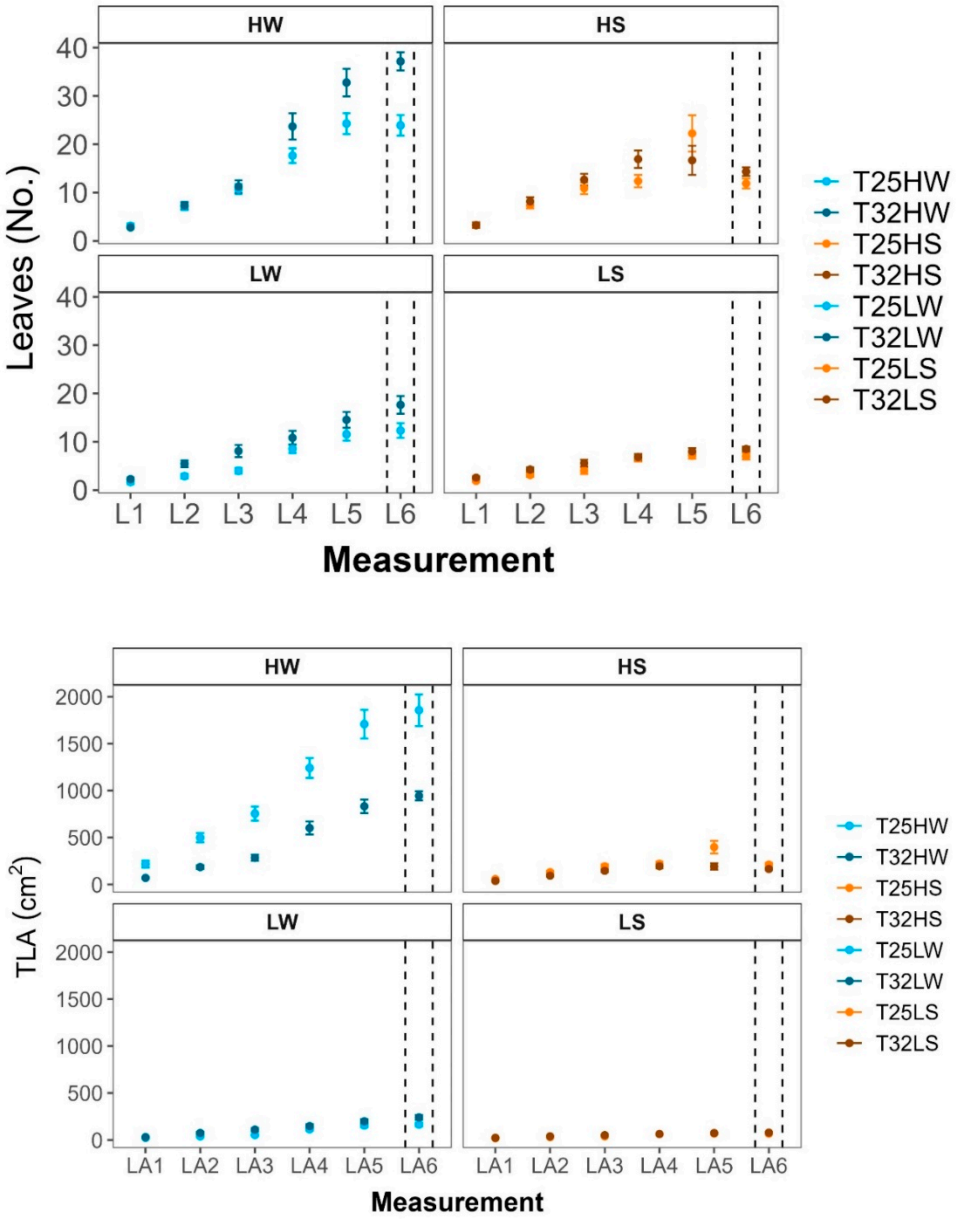

Figure A1. Temporal dynamics of plant morphological traits: **a**) diameter (h, cm), **b**) diameter (d, mm), **c**) leaves number (Leaves, no.), and **d**) Total leaf area (TLA, cm²) measured over six different assessments (h1–h6, d1–d6, L1–L6, and LA1–LA6 respectively) to different treatments: HW (high light well-watered), HS (high light water-stressed), LW (low light well-watered), LS (low light water-stressed) and growth temperatures (T25, T32).. Measurements were conducted on plants grown at two contrasting temperatures (25°C and 32°C). Data points represent means ± standard error (SE). Dashed vertical lines indicate the final measurement point, corresponding to the moment of sampling and measurement for the results discussed in this study.

 doi:10.20944/preprints202504.1808.v1

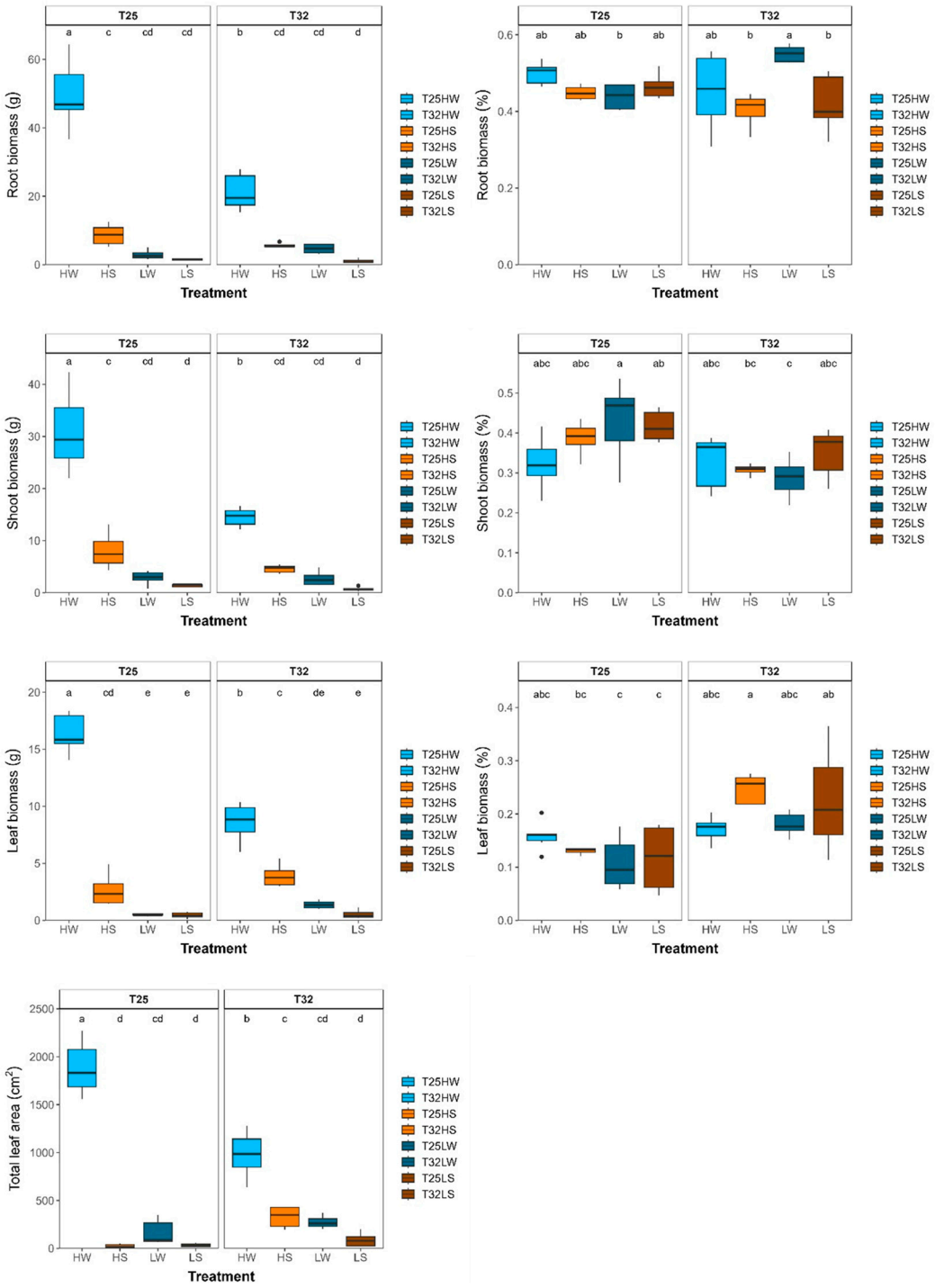

Figure A2. Plasticity of biomass of beech seedlings growing under contrasted temperature, water and light treatments: **a**) absolute root biomass (RB, g); **b**) relative root biomass to total biomass (RB, %); **c**) absolute shoot biomass (SB, g); **d**) relative shoot biomass to total biomass (SB, %); **e)** absolute leaves biomass (LB, g); **f**) relative leaves biomass to total biomass (LB, %) and **g**) total leaf area (TLA, cm^2). Each bar or box plot represent (mean ± SE) under different treatments: HW (high light well-watered), HS (high light water-stressed), LW (low light well-watered), LS (low light water-stressed) and growth temperatures (T25, T32). Each boxplot represents the interquartile range (IQR), with the lower and upper edges corresponding to the first (Q1) and third (Q3) quartiles, respectively. The straight horizontal black line within each box indicates the median. Different letters indicate significant differences among treatments.

 doi:10.20944/preprints202504.1808.v1

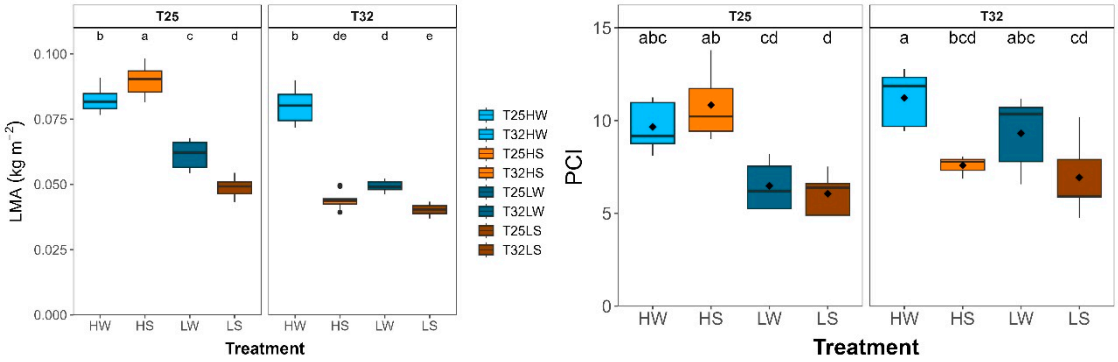

Figure A3. Plasticity of leaf morphological traits of beech seedlings growing under contrasted temperature, water and light treatments: **a**) leaf mass area (LMA, kg m^{-2}); **b**) potential conductance index (PCI). Each bar or box plot represent (mean ± SE) under different treatments: HW (high light well-watered), HS (high light water-stressed), LW (low light well-watered), LS (low light water-stressed) and growth temperatures (T25, T32). Each boxplot represents the interquartile range (IQR), with the lower and upper edges corresponding to the first (Q1) and third (Q3) quartiles, respectively. The straight horizontal black line within each box indicates the median. Different letters indicate significant differences among treatments.

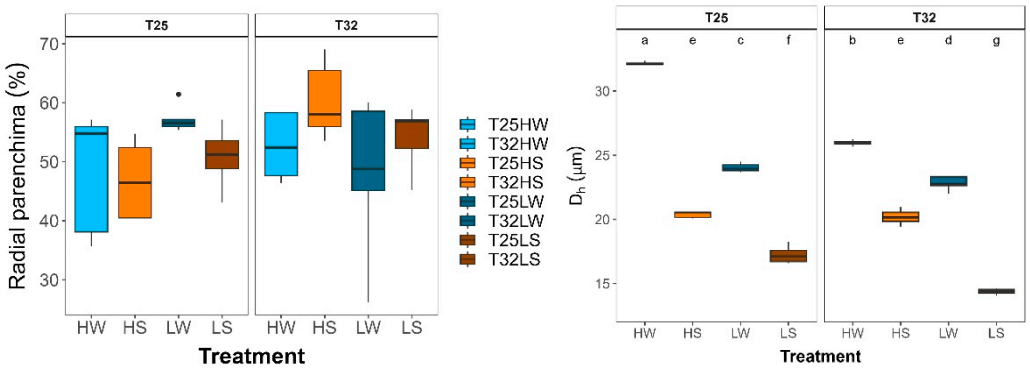

Figure A4. Plasticity of xylem morphological traits of beech seedlings growing under contrasted temperature, water and light treatments: **a**) Xylem area occupied by radial parenchyma (Radial parenchyma, %); **b**) hydraulic diameter (Dh, μm). Each bar or box plot represent (mean ± SE) under different treatments: HW (high light well-watered), HS (high light water-stressed), LW (low light well-watered), LS (low light water-stressed) and growth temperatures (T25, T32). Each boxplot represents the interquartile range (IQR), with the lower and upper edges corresponding to the first (Q1) and third (Q3) quartiles, respectively. The straight horizontal black line within each box indicates the median. Different letters indicate significant differences among treatments.

Preprints.org (www.preprints.org) | NOT PEER-REVIEWED | Posted: 22 April 2025 doi:10.20944/preprints202504.1808.v1

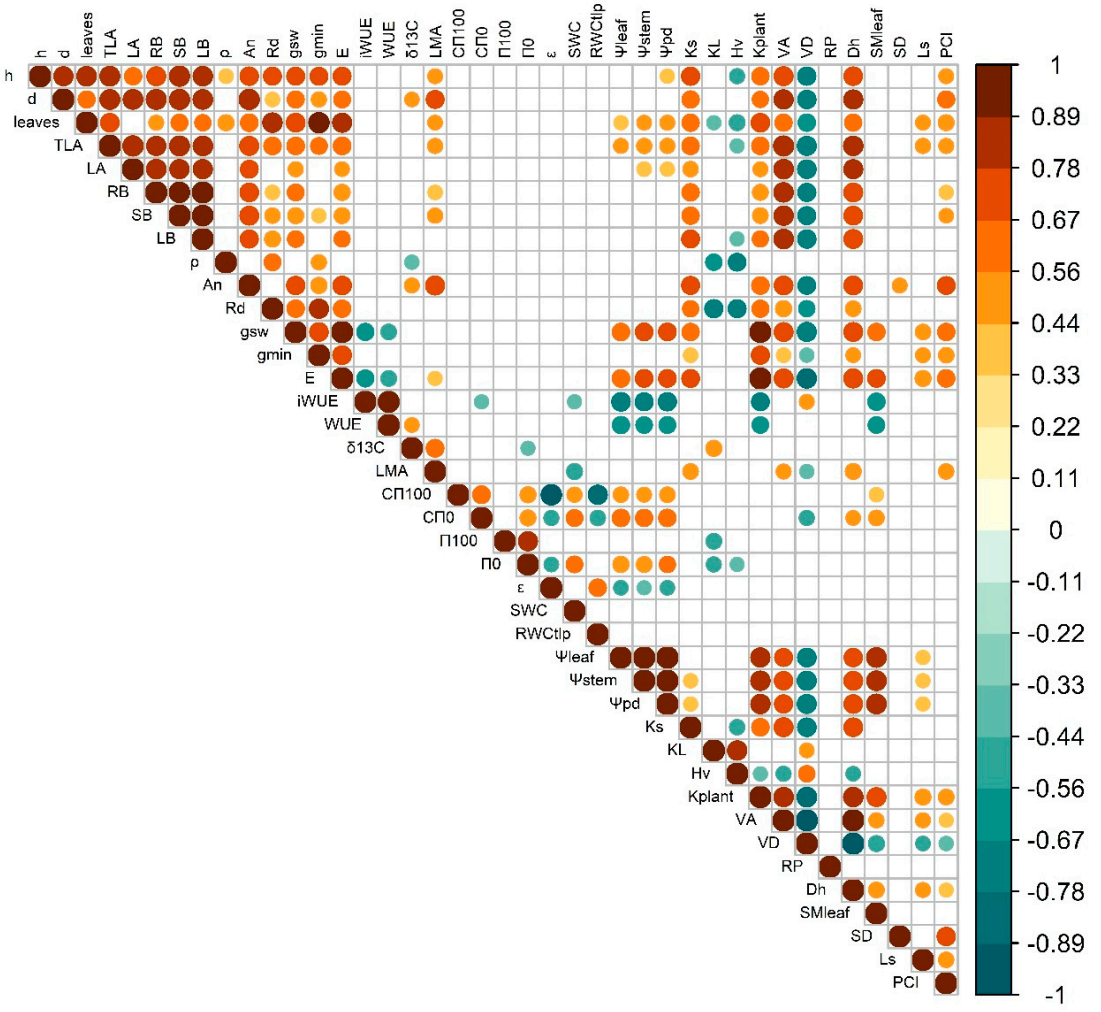

Figure A5. Pearson's correlation matrix for the evaluated traits and all the treatments (including T25 and T32). Significant correlations are colour coded, with positive correlations in warm colours and negative correlations in cool colours. For abbreviations, check Table 1.

 doi:10.20944/preprints202504.1808.v1

Figure A6. Relative response, or plasticity score, of each trait to the effect of each growing factor according to the Phenotypic Plasticity Index (PPI) as described by [173].

References

1. IPCC Summary for Policymakers. In: Climate Change 2023: Synthesis Report.Contribution of Working Groups I, II and III to the Sixth Assessment Report of the Intergovernmental Panel on Climate Change; Lee, H., Romero, J., Eds.; IPCC: Geneva, Switzerland, 2023;

2. Kobe, R.K.; Pacala, S.W.; Silander Jr., J.A.; Canham, C.D. Juvenile Tree Survivorship as a Component of Shade Tolerance. Ecological Applications 1995, 5, 517–532, doi:https://doi.org/10.2307/1942040.
3. Pineda-García, F.; Paz, H.; Meinzer, F.C. Drought Resistance in Early and Late Secondary Successional Species from a Tropical Dry Forest: The Interplay between Xylem Resistance to Embolism, Sapwood Water Storage and Leaf Shedding. Plant Cell Environ 2013, 36, 405–418, doi:https://doi.org/10.1111/j.1365-3040.2012.02582.x.
4. Valladares, F.; Matesanz, S.; Guilhaumon, F.; Araújo, M.B.; Balaguer, L.; Benito-Garzón, M.; Cornwell, W.; Gianoli, E.; van Kleunen, M.; Naya, D.E.; et al. The Effects of Phenotypic Plasticity and Local Adaptation on Forecasts of Species Range Shifts under Climate Change. Ecol Lett 2014, 17, 1351–1364, doi:https://doi.org/10.1111/ele.12348.
5. Benito Garzón, M.; Robson, T.M.; Hampe, A. ΔTraitSDMs: Species Distribution Models That Account for Local Adaptation and Phenotypic Plasticity. New Phytologist 2019, 222, 1757–1765, doi:https://doi.org/10.1111/nph.15716.
6. Ramírez-Valiente, J.A.; González-Martínez, S.C.; Robledo-Arnuncio, J.J.; Matesanz, S.; Anadon-Rosell, A.; Martínez-Vilalta, J.; López, R.; Cano-Martín, F.J. Genetically Based Trait Coordination and Phenotypic Plasticity of Growth, Gas Exchange, Allometry, and Hydraulics across the Distribution Range of Pinus Pinaster. New Phytologist 2025, 246, 984–1000, doi:https://doi.org/10.1111/nph.70055.
7. Reich, P.B. The World-Wide 'Fast–Slow' Plant Economics Spectrum: A Traits Manifesto. Journal of Ecology 2014, 102, 275–301, doi:https://doi.org/10.1111/1365-2745.12211.
8. Pavanetto, N.; P. Carmona, C.; Laanisto, L.; Niinemets, Ü.; Puglielli, G. Trait Dimensions of Abiotic Stress Tolerance in Woody Plants of the Northern Hemisphere. Global Ecology and Biogeography 2023, 33, doi:10.1111/geb.13788.
9. Valladares, F.; Niinemets, Ü. Shade Tolerance, a Key Plant Feature of Complex Nature and Consequences. Annu Rev Ecol Evol Syst 2008, 39, 237–257, doi:10.1146/annurev.ecolsys.39.110707.173506.
10. Arroyo, J.I.; Díez, B.; Kempes, C.P.; West, G.B.; Marquet, P.A. A General Theory for Temperature Dependence in Biology. Proceedings of the National Academy of Sciences 2022, 119, e2119872119, doi:10.1073/pnas.2119872119.
11. Kumarathunge, D.P.; Drake, J.E.; Tjoelker, M.G.; López, R.; Pfautsch, S.; Vårhammar, A.; Medlyn, B.E. The Temperature Optima for Tree Seedling Photosynthesis and Growth Depend on Water Inputs. Glob Chang Biol 2020, 26, 2544–2560, doi:https://doi.org/10.1111/gcb.14975.
12. Way, D.A.; Oren, R. Differential Responses to Changes in Growth Temperature between Trees from Different Functional Groups and Biomes: A Review and Synthesis of Data. Tree Physiol 2010, 30, 669–688, doi:10.1093/treephys/tpq015.
13. Reich, P.B.; Sendall, K.M.; Rice, K.; Rich, R.L.; Stefanski, A.; Hobbie, S.E.; Montgomery, R.A. Geographic Range Predicts Photosynthetic and Growth Response to Warming in Co-Occurring Tree Species. Nat Clim Chang 2015, 5, 148–152, doi:10.1038/nclimate2497.
14. Yamori, W.; Hikosaka, K.; Way, D.A. Temperature Response of Photosynthesis in C3, C4, and CAM Plants: Temperature Acclimation and Temperature Adaptation. Photosynth Res 2014, 119, 101–117, doi:10.1007/s11120-013-9874-6.
15. Dai, L.; Xu, Y.; Harmens, H.; Duan, H.; Feng, Z.; Hayes, F.; Sharps, K.; Radbourne, A.; Tarvainen, L. Reduced Photosynthetic Thermal Acclimation Capacity under Elevated Ozone in Poplar (Populus Tremula) Saplings. Glob Chang Biol 2021, 27, 2159–2173, doi:https://doi.org/10.1111/gcb.15564.
16. Atkin, O.K.; Tjoelker, M.G. Thermal Acclimation and the Dynamic Response of Plant Respiration to Temperature. Trend Plant Sci 2003, 8, doi:10.1016/S1360-1385(03)00136-5.
17. Poorter, H.; Niinemets, Ü.; Poorter, L.; Wright, I.J.; Villar, R. Causes and Consequences of Variation in Leaf Mass per Area (LMA): A Meta-Analysis. New Phytologist 2009, 182, 565–588, doi:https://doi.org/10.1111/j.1469-8137.2009.02830.x.
18. Westoby, M.; Falster, D.S.; Moles, A.T.; Vesk, P.A.; Wright, I.J. Plant Ecological Strategies: Some Leading Dimensions of Variation Between Species. Annu Rev Ecol Evol Syst 2002, 33, 125–159, doi:https://doi.org/10.1146/annurev.ecolsys.33.010802.150452.

 doi:10.20944/preprints202504.1808.v1

19. Wright, I.; Reich, P.; Westoby, M.; Ackerly, D.; Baruch, Z.; Bongers, F.; Cavender-Bares, J.; Cornelissen, J.; Diemer, M.; Flexas, J.; et al. The World-Wide Leaf Economics Spectrum. Nature 2004, 428, 821–827, doi:10.1038/nature02403.
20. Marchin, R.M.; Backes, D.; Ossola, A.; Leishman, M.R.; Tjoelker, M.G.; Ellsworth, D.S. Extreme Heat Increases Stomatal Conductance and Drought-Induced Mortality Risk in Vulnerable Plant Species. Glob Chang Biol 2022, 28, 1133–1146, doi:https://doi.org/10.1111/gcb.15976.
21. Leigh, A.; Sevanto, S.; Close, J.D.; Nicotra, A.B. The Influence of Leaf Size and Shape on Leaf Thermal Dynamics: Does Theory Hold up under Natural Conditions? Plant Cell Environ 2017, 40, 237–248, doi:https://doi.org/10.1111/pce.12857.
22. Pan, L.; George-Jaeggli, B.; Borrell, A.; Jordan, D.; Koller, F.; Al-Salman, Y.; Ghannoum, O.; Cano, F.J. Coordination of Stomata and Vein Patterns with Leaf Width Underpins Water-Use Efficiency in a C4 Crop. Plant Cell Environ 2022, 45, 1612–1630, doi:https://doi.org/10.1111/pce.14225.
23. Crous, K.Y.; Uddling, J.; De Kauwe, M.G. Temperature Responses of Photosynthesis and Respiration in Evergreen Trees from Boreal to Tropical Latitudes. New Phytologist 2022, 234, 353–374, doi:https://doi.org/10.1111/nph.17951.
24. Reich, P.; Sendall, K.; Stefanski, A.; Wei, X.; Rich, R.; Montgomery, R. Boreal and Temperate Trees Show Strong Acclimation of Respiration to Warming. Nature 2016, 531, doi:10.1038/nature17142.
25. Ghannoum, O.; Phillips, N.; SEARS, M.; LOGAN, B.; Lewis, J.; Conroy, J.; Tissue, D. Photosynthetic Responses of Two Eucalypts to Industrial-Age Changes in Atmospheric [CO2] and Temperature: Eucalyptus Photosynthesis in Past and Future Climates. Plant Cell and Environment - PLANT CELL ENVIRON 2010.
26. Kumarathunge, D.P.; Medlyn, B.E.; Drake, J.E.; Tjoelker, M.G.; Aspinwall, M.J.; Battaglia, M.; Cano, F.J.; Carter, K.R.; Cavaleri, M.A.; Cernusak, L.A.; et al. Acclimation and Adaptation Components of the Temperature Dependence of Plant Photosynthesis at the Global Scale. New Phytologist 2019, 222, 768–784, doi:https://doi.org/10.1111/nph.15668.
27. Smith, N.G.; Dukes, J.S. Plant Respiration and Photosynthesis in Global-Scale Models: Incorporating Acclimation to Temperature and 2. Glob Chang Biol 2013, 19, 45–63, doi:https://doi.org/10.1111/j.1365-2486.2012.02797.x.
28. Urban, J.; Ingwers, M.; McGuire, M.A.; Teskey, R.O. Stomatal Conductance Increases with Rising Temperature. Plant Signal Behav 2017, 12, e1356534, doi:10.1080/15592324.2017.1356534.
29. Drake, J.E.; Tjoelker, M.G.; Vårhammar, A.; Medlyn, B.E.; Reich, P.B.; Leigh, A.; Pfautsch, S.; Blackman, C.J.; López, R.; Aspinwall, M.J.; et al. Trees Tolerate an Extreme Heatwave via Sustained Transpirational Cooling and Increased Leaf Thermal Tolerance. Glob Chang Biol 2018, 24, 2390–2402, doi:https://doi.org/10.1111/gcb.14037.
30. De Kauwe, M.G.; Medlyn, B.E.; Pitman, A.J.; Drake, J.E.; Ukkola, A.; Griebel, A.; Pendall, E.; Prober, S.; Roderick, M. Examining the Evidence for Decoupling between Photosynthesis and transpiration during Heat Extremes. Biogeosciences 2019, 16, 903–916, doi:10.5194/bg-16-903-2019.
31. Feng, X.; Liu, R.; Li, C.; Zhang, H.; Slot, M. Contrasting Responses of Two C4 Desert Shrubs to Drought but Consistent Decoupling of Photosynthesis and Stomatal Conductance at High Temperature. Environ Exp Bot 2023, 209, 105295, doi:https://doi.org/10.1016/j.envexpbot.2023.105295.
32. Diao, H.; Cernusak, L.A.; Saurer, M.; Gessler, A.; Siegwolf, R.T.W.; Lehmann, M.M. Uncoupling of Stomatal Conductance and Photosynthesis at High Temperatures: Mechanistic Insights from Online Stable Isotope Techniques. New Phytologist 2024, 241, 2366–2378, doi:https://doi.org/10.1111/nph.19558.
33. Schönbeck, L.C.; Schuler, P.; Lehmann, M.M.; Mas, E.; Mekarni, L.; Pivovaroff, A.L.; Turberg, P.; Grossiord, C. Increasing Temperature and Vapour Pressure Deficit Lead to Hydraulic Damages in the Absence of Soil Drought. Plant Cell Environ 2022, 45, 3275–3289, doi:https://doi.org/10.1111/pce.14425.
34. Ogren, W.L. Photorespiration: Pathways, Regulation, And. Annu Rev Plant Biol 1984, 35, 415–442, doi:https://doi.org/10.1146/annurev.pp.35.060184.002215.
35. Suzuki, N.; Mittler, R. Reactive Oxygen Species and Temperature Stresses: A Delicate Balance between Signaling and Destruction. Physiol Plant 2006, 126, 45–51, doi:https://doi.org/10.1111/j.0031-9317.2005.00582.x.

 doi:10.20944/preprints202504.1808.v1

36. Hetherington, A.M.; Woodward, F.I. The Role of Stomata in Sensing and Driving Environmental Change. Nature 2003, 424, 901–908, doi:10.1038/nature01843.
37. Franks, P.; Brodribb, T. Stomatal Control and Water Transport in the Xylem. In Vascular Transport in Plants; 2005; pp. 69–89 ISBN 9780120884575.
38. Choat, B.; Brodribb, T.J.; Brodersen, C.R.; Duursma, R.A.; López, R.; Medlyn, B.E. Triggers of Tree Mortality under Drought. Nature 2018, 558, 531–539, doi:10.1038/s41586-018-0240-x.
39. Mantova, M.; Cochard, H.; Burlett, R.; Delzon, S.; King, A.; Rodriguez-Dominguez, C.M.; Ahmed, M.A.; Trueba, S.; Torres-Ruiz, J.M. On the Path from Xylem Hydraulic Failure to Downstream Cell Death. New Phytologist 2023, 237, 793–806, doi:https://doi.org/10.1111/nph.18578.
40. Grossiord, C.; Sevanto, S.; Borrego, I.; Chan, A.M.; Collins, A.D.; Dickman, L.T.; Hudson, P.J.; McBranch, N.; Michaletz, S.T.; Pockman, W.T.; et al. Tree Water Dynamics in a Drying and Warming World. Plant Cell Environ 2017, 40, 1861–1873, doi:https://doi.org/10.1111/pce.12991.
41. Way, D.A.; Domec, J.-C.; Jackson, R.B. Elevated Growth Temperatures Alter Hydraulic Characteristics in Trembling Aspen (Populus Tremuloides) Seedlings: Implications for Tree Drought Tolerance. Plant Cell Environ 2013, 36, 103–115, doi:https://doi.org/10.1111/j.1365-3040.2012.02557.x.
42. Bartlett, M.K.; Scoffoni, C.; Sack, L. The Determinants of Leaf Turgor Loss Point and Prediction of Drought Tolerance of Species and Biomes: A Global Meta-Analysis. Ecol Lett 2012, 15, 393–405, doi:https://doi.org/10.1111/j.1461-0248.2012.01751.x.
43. López, J.; Way, D.A.; Sadok, W. Systemic Effects of Rising Atmospheric Vapor Pressure Deficit on Plant Physiology and Productivity. Glob Chang Biol 2021, 27, 1704–1720, doi:https://doi.org/10.1111/gcb.15548.
44. Aranda, I.; Cadahía, E.; Fernández de Simón, B. Specific Leaf Metabolic Changes That Underlie Adjustment of Osmotic Potential in Response to Drought by Four Quercus Species. Tree Physiol 2021, 41, 728–743, doi:10.1093/treephys/tpaa157.
45. Maherali, H.; DeLucia, E.H. Xylem Conductivity and Vulnerability to Cavitation of Ponderosa Pine Growing in Contrasting Climates. Tree Physiol 2000, 20, 859–867, doi:10.1093/treephys/20.13.859.
46. McCulloh, K.A.; Petitmermet, J.; Stefanski, A.; Rice, K.E.; Rich, R.L.; Montgomery, R.A.; Reich, P.B. Is It Getting Hot in Here? Adjustment of Hydraulic Parameters in Six Boreal and Temperate Tree Species after 5 Years of Warming. Glob Chang Biol 2016, 22, 4124–4133, doi:https://doi.org/10.1111/gcb.13323.
47. Thomas, D.S.; Montagu, K.D.; Conroy, J.P. Changes in Wood Density of Eucalyptus Camaldulensis Due to Temperature—the Physiological Link between Water Viscosity and Wood Anatomy. For Ecol Manage 2004, 193, 157–165, doi:https://doi.org/10.1016/j.foreco.2004.01.028.
48. Thomas, D.S.; Montagu, K.D.; Conroy, J.P. Temperature Effects on Wood Anatomy, Wood Density, Photosynthesis and Biomass Partitioning of Eucalyptus Grandis Seedlings. Tree Physiol 2007, 27, 251–260, doi:10.1093/treephys/27.2.251.
49. Sellin, A.; Kupper, P. Temperature, Light and Leaf Hydraulic Conductance of Little-Leaf Linden (Tilia Cordata) in a Mixed Forest Canopy. Tree Physiol 2007, 27, 679–688, doi:10.1093/treephys/27.5.679.
50. Bowman, D.; French, B.; Prior, L. Have Plants Evolved to Self-Immolate? Front Plant Sci 2014, 5, 590, doi:10.3389/fpls.2014.00590.
51. Duan, H.; Amthor, J.S.; Duursma, R.A.; O'Grady, A.P.; Choat, B.; Tissue, D.T. Carbon Dynamics of Eucalypt Seedlings Exposed to Progressive Drought in Elevated [CO2] and Elevated Temperature. Tree Physiol 2013, 33, 779–792, doi:10.1093/treephys/tpt061.
52. Rodríguez-Calcerrada, J.; Atkin, O.K.; Robson, T.M.; Zaragoza-Castells, J.; Gil, L.; Aranda, I. Thermal Acclimation of Leaf Dark Respiration of Beech Seedlings Experiencing Summer Drought in High and Low Light Environments. Tree Physiol 2010, 30, 214–224, doi:10.1093/treephys/tpp104.
53. Osonubi, O.; Davies, W.J. The Influence of Water Stress on the Photosynthetic Performance and Stomatal Behaviour of Tree Seedlings Subjected to Variation in Temperature and Irradiance. Oecologia 1980, 45, 3–10, doi:10.1007/BF00346699.
54. Cano, F.J.; Sánchez-Gómez, D.; Rodríguez-Calcerrada, J.; Warren, C.R.; Gil, L.; Aranda, I. Effects of Drought on Mesophyll Conductance and Photosynthetic Limitations at Different Tree Canopy Layers. Plant Cell Environ 2013, 36, 1961–1980, doi:https://doi.org/10.1111/pce.12103.

 doi:10.20944/preprints202504.1808.v1

55. Cano, F.J.; López, R.; Warren, C.R. Implications of the Mesophyll Conductance to CO2 for Photosynthesis and Water-Use Efficiency during Long-Term Water Stress and Recovery in Two Contrasting Eucalyptus Species. Plant Cell Environ 2014, 37, 2470–2490, doi:https://doi.org/10.1111/pce.12325.
56. Bartlett, M.K.; Scoffoni, C.; Ardy, R.; Zhang, Y.; Sun, S.; Cao, K.; Sack, L. Rapid Determination of Comparative Drought Tolerance Traits: Using an Osmometer to Predict Turgor Loss Point. Methods Ecol Evol 2012, 3, 880–888, doi:https://doi.org/10.1111/j.2041-210X.2012.00230.x.
57. Al-Salman, Y.; Ghannoum, O.; Cano, F.J. Elevated [CO2] Negatively Impacts C4 Photosynthesis under Heat and Water Stress without Penalizing Biomass. J Exp Bot 2023, 74, 2875–2890, doi:10.1093/jxb/erad063.
58. Cochard, H.; Pimont, F.; Ruffault, J.; Martin-StPaul, N. SurEau: A Mechanistic Model of Plant Water Relations under Extreme Drought. Ann For Sci 2021, 78, 55, doi:10.1007/s13595-021-01067-y.
59. López, R.; Cano, F.J.; Martin-StPaul, N.K.; Cochard, H.; Choat, B. Coordination of Stem and Leaf Traits Define Different Strategies to Regulate Water Loss and Tolerance Ranges to Aridity. New Phytologist 2021, 230, 497–509, doi:https://doi.org/10.1111/nph.17185.
60. 60. Schuster, A.-C.; Burghardt, M.; Alfarhan, A.; Bueno, A.; Hedrich, R.; Leide, J.; Thomas, J.; Riederer, M. Effectiveness of Cuticular Transpiration Barriers in a Desert Plant at Controlling Water Loss at High Temperatures. AoB Plants 2016, 8, plw027, doi:10.1093/aobpla/plw027.
61. Duursma, R.A.; Blackman, C.J.; Lopéz, R.; Martin-StPaul, N.K.; Cochard, H.; Medlyn, B.E. On the Minimum Leaf Conductance: Its Role in Models of Plant Water Use, and Ecological and Environmental Controls. New Phytologist 2019, 221, 693–705, doi:https://doi.org/10.1111/nph.15395.
62. Bueno, A.; Alfarhan, A.; Arand, K.; Burghardt, M.; Deininger, A.-C.; Hedrich, R.; Leide, J.; Seufert, P.; Staiger, S.; Riederer, M. Effects of Temperature on the Cuticular Transpiration Barrier of Two Desert Plants with Water-Spender and Water-Saver Strategies. J Exp Bot 2019, 70, 1613–1625, doi:10.1093/jxb/erz018.
63. Vergarechea, M.; del Río, M.; Gordo, J.; Martín, R.; Cubero, D.; Calama, R. Spatio-Temporal Variation of Natural Regeneration in Pinus Pinea and Pinus Pinaster Mediterranean Forests in Spain. Eur J For Res 2019, 138, 313–326, doi:10.1007/s10342-019-01172-8.
64. Hamerlynck, E.; Knapp, A.K. Photosynthetic and Stomatal Responses to High Temperature and Light in Two Oaks at the Western Limit of Their Range. Tree Physiol 1996, 16, 557–565, doi:10.1093/treephys/16.6.557.
65. Küppers, M.; Schneider, H. Leaf Gas Exchange of Beech (Fagus Sylvatica L.) Seedlings in Lightflecks: Effects of Fleck Length and Leaf Temperature in Leaves Grown in Deep and Partial Shade. Trees 1993, 7, 160–168, doi:10.1007/BF00199617.
66. Bachofen, C.; D'Odorico, P.; Buchmann, N. Light and VPD Gradients Drive Foliar Nitrogen Partitioning and Photosynthesis in the Canopy of European Beech and Silver Fir. Oecologia 2020, 192, 323–339, doi:10.1007/s00442-019-04583-x.
67. Salah, H.B.H.; Tardieu, F. Quantitative Analysis of the Combined Effects of Temperature, Evaporative Demand and Light on Leaf Elongation Rate in Well-Watered Field and Laboratory-Grown Maize Plants. J Exp Bot 1996, 47, 1689–1698, doi:10.1093/jxb/47.11.1689.
68. Chapin III, F.S.; Bloom, A.J.; Field, C.B.; Waring, R.H. Plant Responses to Multiple Environmental Factors: Physiological Ecology Provides Tools for Studying How Interacting Environmental Resources Control Plant Growth. Bioscience 1987, 37, 49–57, doi:10.2307/1310177.
69. Valladares, F.; Pearcy, R.W. Drought Can Be More Critical in the Shade than in the Sun: A Field Study of Carbon Gain and Photo-Inhibition in a Californian Shrub during a Dry El Niño Year. Plant Cell Environ 2002, 25, 749–759, doi:10.1046/j.1365-3040.2002.00856.x.
70. Aranda, I.; Robson, T.; Rodríguez-Calcerrada, J.; Valladares, F. Limited Capacity to Cope with Excessive Light in the Open and with Seasonal Drought in the Shade in Mediterranean Ilex Aquifolium Populations. Trees 2008, 22, 375–384, doi:10.1007/s00468-007-0192-5.
71. Aranda, I.; Gil, L.; Pardos, J. Effects of Thinning in a Pinus Sylvestris L. Stand on Foliar Water Relations of Fagus Sylvatica L. Seedlings Planted within the Pinewood. Trees 2001, 15, 358–364, doi:10.1007/s004680100109.

 doi:10.20944/preprints202504.1808.v1

72. Aranda, I.; Gil, L.; Pardos, J.A. Physiological Responses of Fagus Sylvatica L. Seedlings under Pinus Sylvestris L. and Quercus Pyrenaica Willd. Overstories. For Ecol Manage 2002, 162, 153–164, doi:https://doi.org/10.1016/S0378-1127(01)00502-3.
73. Fortunel, C.; Garnier, E.; Joffre, R.; Kazakou, E.; Quested, H.; Grigulis, K.; Lavorel, S.; Ansquer, P.; Castro, H.; Cruz, P.; et al. Leaf Traits Capture the Effects of Land Use Changes and Climate on Litter Decomposability of Grasslands across Europe. Ecology 2009, 90, 598–611, doi:https://doi.org/10.1890/08-0418.1.
74. Tschaplinski, T.J.; Gebre, G.M.; Shirshac, T.L. Osmotic Potential of Several Hardwood Species as Affected by Manipulation of Throughfall Precipitation in an Upland Oak Forest during a Dry Year. Tree Physiol 1998, 18, 291–298, doi:10.1093/treephys/18.5.291.
75. Niinemets, Ü. Global-Scale Climatic Controls of Leaf Dry Mass per Area, Density, and Thickness in Trees and Shrubs. Ecology 2001, 82, 453–469, doi:10.1890/0012-9658(2001)082[0453:GSCCOL]2.0.CO;2.
76. Aranda, I.; Bergasa, L.F.; Gil, L.; Pardos, J.A. Effects of Relative Irradiance on the Leaf Structure of Fagus Sylvatica L. Seedlings Planted in the Understory of a Pinus Sylvestris L. Stand after Thinning. Ann. For. Sci. 2001, 58, 673–680.
77. Rodríguez-Calcerrada, J.; Pardos, J.A.; Gil, L.; Aranda, I. Ability to Avoid Water Stress in Seedlings of Two Oak Species Is Lower in a Dense Forest Understory than in a Medium Canopy Gap. For Ecol Manage 2008, 255, 421–430, doi:https://doi.org/10.1016/j.foreco.2007.09.009.
78. Sharkey, T.D. Effects of Moderate Heat Stress on Photosynthesis: Importance of Thylakoid Reactions, Rubisco Deactivation, Reactive Oxygen Species, and Thermotolerance Provided by Isoprene. Plant Cell Environ 2005, 28, doi:10.1111/j.1365-3040.2005.01324.x.
79. Weston, D.J.; Bauerle, W.L. Inhibition and Acclimation of C3 Photosynthesis to Moderate Heat: A Perspective from Thermally Contrasting Genotypes of Acer Rubrum (Red Maple). Tree Physiol 2007, 27, 1083–1092, doi:10.1093/treephys/27.8.1083.
80. Salvucci, M.E.; Crafts-Brandner, S.J. Mechanism for Deactivation of Rubisco under Moderate Heat Stress. Physiol Plant 2004, 122, doi:10.1111/j.1399-3054.2004.00419.x.
81. Ciais, Ph.; Reichstein, M.; Viovy, N.; Granier, A.; Ogée, J.; Allard, V.; Aubinet, M.; Buchmann, N.; Bernhofer, Chr.; Carrara, A.; et al. Europe-Wide Reduction in Primary Productivity Caused by the Heat and Drought in 2003. Nature 2005, 437, 529–533, doi:10.1038/nature03972.
82. Jumrani, K.; Bhatia, V.S. Interactive Effect of Temperature and Water Stress on Physiological and Biochemical Processes in Soybean. Physiology and Molecular Biology of Plants 2019, 25, 667–681, doi:10.1007/s12298-019-00657-5.
83. Mittler, R. Abiotic Stress, the Field Environment and Stress Combination. Trends Plant Sci 2006, 11, 15–19, doi:10.1016/j.tplants.2005.11.002.
84. Suzuki, N.; Rivero, R.M.; Shulaev, V.; Blumwald, E.; Mittler, R. Abiotic and Biotic Stress Combinations. New Phytologist 2014, 203, 32–43, doi:https://doi.org/10.1111/nph.12797.
85. Zandalinas, S.I.; Mittler, R. Plant Responses to Multifactorial Stress Combination. New Phytologist 2022, 234, 1161–1167, doi:https://doi.org/10.1111/nph.18087.
86. Yang, Z.; Sinclair, T.R.; Zhu, M.; Messina, C.D.; Cooper, M.; Hammer, G.L. Temperature Effect on Transpiration Response of Maize Plants to Vapour Pressure Deficit. Environ Exp Bot 2012, 78, 157–162, doi:https://doi.org/10.1016/j.envexpbot.2011.12.034.
87. Sadok, W.; Lopez, J.R.; Smith, K.P. Transpiration Increases under High-Temperature Stress: Potential Mechanisms, Trade-Offs and Prospects for Crop Resilience in a Warming World. Plant Cell Environ 2021, 44, 2102–2116, doi:https://doi.org/10.1111/pce.13970.
88. Choudhary, S.; Guha, A.; Kholova, J.; Pandravada, A.; Messina, C.D.; Cooper, M.; Vadez, V. Maize, Sorghum, and Pearl Millet Have Highly Contrasting Species Strategies to Adapt to Water Stress and Climate Change-like Conditions. Plant Science 2020, 295, 110297, doi:https://doi.org/10.1016/j.plantsci.2019.110297.
89. Seversike, T.M.; Sermons, S.M.; Sinclair, T.R.; Carter Jr, T.E.; Rufty, T.W. Temperature Interactions with Transpiration Response to Vapor Pressure Deficit among Cultivated and Wild Soybean Genotypes. Physiol Plant 2013, 148, 62–73, doi:https://doi.org/10.1111/j.1399-3054.2012.01693.x.

90. Riar, M.K.; Sinclair, T.R.; Prasad, P.V.V. Persistence of Limited-Transpiration-Rate Trait in Sorghum at High Temperature. Environ Exp Bot 2015, 115, 58–62, doi:https://doi.org/10.1016/j.envexpbot.2015.02.007.
91. Koehler, T.; Wankmüller, F.J.P.; Sadok, W.; Carminati, A. Transpiration Response to Soil Drying versus Increasing Vapor Pressure Deficit in Crops: Physical and Physiological Mechanisms and Key Plant Traits. J Exp Bot 2023, 74, 4789–4807, doi:10.1093/jxb/erad221.
92. Mills, C.; Bartlett, M.; Buckley, T. The Poorly-Explored Stomatal Response to Temperature at Constant Evaporative Demand. Plant Cell Environ 2024, 47, doi:10.1111/pce.14911.
93. Zandalinas, S.I.; Sengupta, S.; Fritschi, F.B.; Azad, R.K.; Nechushtai, R.; Mittler, R. The Impact of Multifactorial Stress Combination on Plant Growth and Survival. New Phytologist 2021, 230, 1034–1048, doi:https://doi.org/10.1111/nph.17232.
94. Zandalinas, S.I.; Peláez-Vico, M.Á.; Sinha, R.; Pascual, L.S.; Mittler, R. The Impact of Multifactorial Stress Combination on Plants, Crops, and Ecosystems: How Should We Prepare for What Comes Next? The Plant Journal 2024, 117, 1800–1814, doi:https://doi.org/10.1111/tpj.16557.
95. Reich, P.B.; Oleksyn, J. Climate Warming Will Reduce Growth and Survival of Scots Pine except in the Far North. Ecol Lett 2008, 11, 588–597, doi:https://doi.org/10.1111/j.1461-0248.2008.01172.x.
96. Wertin, T.M.; McGuire, M.A.; Teskey, R.O. Higher Growth Temperatures Decreased Net Carbon Assimilation and Biomass Accumulation of Northern Red Oak Seedlings near the Southern Limit of the Species Range. Tree Physiol 2011, 31, 1277–1288, doi:10.1093/treephys/tpr091.
97. Van Gelder, H.A.; Poorter, L.; Sterck, F.J. Wood Mechanics, Allometry, and Life-History Variation in a Tropical Rain Forest Tree Community. New Phytologist 2006, 171, 367–378, doi:https://doi.org/10.1111/j.1469-8137.2006.01757.x.
98. Hacke, U.G.; Sperry, J.S.; Pockman, W.T.; Davis, S.D.; McCulloh, K.A. Trends in Wood Density and Structure Are Linked to Prevention of Xylem Implosion by Negative Pressure. Oecologia 2001, 126, 457–461, doi:10.1007/s004420100628.
99. Sperry, J. Evolution of Water Transport and Xylem Structure. Int J Plant Sci 164:S115-S127. Int J Plant Sci 2003, 164, doi:10.1086/368398.
100. Roderick, M.L.; Berry, S.L. Linking Wood Density with Tree Growth and Environment: A Theoretical Analysis Based on the Motion of Water. New Phytologist 2001, 149, 473–485, doi:https://doi.org/10.1046/j.1469-8137.2001.00054.x.
101. Cochard, H.; Martin, R.; Gross, P.; Bogeat-Triboulot, M.B. Temperature Effects on Hydraulic Conductance and Water Relations of Quercus Robur L. J Exp Bot 2000, 51, 1255–1259, doi:10.1093/jexbot/51.348.1255.
102. Meier, I.C.; Leuschner, C. Leaf Size and Leaf Area Index in Fagus Sylvatica Forests: Competing Effects of Precipitation, Temperature, and Nitrogen Availability. Ecosystems 2008, 11, 655–669, doi:10.1007/s10021-008-9135-2.
103. Jin, B.; Wang, L.; Wang, J.; Jiang, K.-Z.; Wang, Y.; Jiang, X.-X.; Ni, C.-Y.; Wang, Y.-L.; Teng, N.-J. The Effect of Experimental Warming on Leaf Functional Traits, Leaf Structure and Leaf Biochemistry in Arabidopsis Thaliana. BMC Plant Biol 2011, 11, 35, doi:10.1186/1471-2229-11-35.
104. Gates, D.M. Transpiration and Leaf Temperature. Annu Rev Plant Biol 1968, 19, 211–238, doi:https://doi.org/10.1146/annurev.pp.19.060168.001235.
105. Blasini, D.E.; Koepke, D.F.; Bush, S.E.; Allan, G.J.; Gehring, C.A.; Whitham, T.G.; Day, T.A.; Hultine, K.R. Tradeoffs between Leaf Cooling and Hydraulic Safety in a Dominant Arid Land Riparian Tree Species. Plant Cell Environ 2022, 45, 1664–1681, doi:https://doi.org/10.1111/pce.14292.
106. Poorter, L.; McDonald, I.; Alarcón, A.; Fichtler, E.; Licona, J.-C.; Peña-Claros, M.; Sterck, F.; Villegas, Z.; Sass-Klaassen, U. The Importance of Wood Traits and Hydraulic Conductance for the Performance and Life History Strategies of 42 Rainforest Tree Species. New Phytologist 2010, 185, 481–492, doi:https://doi.org/10.1111/j.1469-8137.2009.03092.x.
107. Mencuccini, M.; Rosas, T.; Rowland, L.; Choat, B.; Cornelissen, H.; Jansen, S.; Kramer, K.; Lapenis, A.; Manzoni, S.; Niinemets, Ü.; et al. Leaf Economics and Plant Hydraulics Drive Leaf : Wood Area Ratios. New Phytologist 2019, 224, 1544–1556, doi:https://doi.org/10.1111/nph.15998.
108. Joshi, J.; Stocker, B.D.; Hofhansl, F.; Zhou, S.; Dieckmann, U.; Prentice, I.C. Towards a Unified Theory of Plant Photosynthesis and Hydraulics. Nat Plants 2022, 8, 1304–1316, doi:10.1038/s41477-022-01244-5.

 doi:10.20944/preprints202504.1808.v1

109. Šigut, L.; Holišová, P.; Klem, K.; Šprtová, M.; Calfapietra, C.; Marek, M. V; Špunda, V.; Urban, O. Does Long-Term Cultivation of Saplings under Elevated CO2 Concentration Influence Their Photosynthetic Response to Temperature? Ann Bot 2015, 116, 929–939, doi:10.1093/aob/mcv043.
110. Chaves, M.; Maroco, J.; Pereira, J. Understanding Plant Responses to Drought - From Genes to the Whole Plant. Functional Plant Biology - FUNCT PLANT BIOL 2003, 30, doi:10.1071/FP02076.
111. Ameye, M.; Wertin, T.M.; Bauweraerts, I.; McGuire, M.A.; Teskey, R.O.; Steppe, K. The Effect of Induced Heat Waves on Inus Taeda and Uercus Rubra Seedlings in Ambient and Elevated CO2 Atmospheres. New Phytologist 2012, 196, 448–461, doi:https://doi.org/10.1111/j.1469-8137.2012.04267.x.
112. Didion-Gency, M.; Vitasse, Y.; Buchmann, N.; Gessler, A.; Gisler, J.; Schaub, M.; Grossiord, C. Chronic Warming and Dry Soils Limit Carbon Uptake and Growth despite a Longer Growing Season in Beech and Oak. Plant Physiol 2024, 194, 741–757, doi:10.1093/plphys/kiad565.
113. Duan, H.; O'Grady, A.P.; Duursma, R.A.; Choat, B.; Huang, G.; Smith, R.A.; Jiang, Y.; Tissue, D.T. Drought Responses of Two Gymnosperm Species with Contrasting Stomatal Regulation Strategies under Elevated [CO2] and Temperature. Tree Physiol 2015, 35, 756–770, doi:10.1093/treephys/tpv047.
114. Blasini, D.E.; Koepke, D.F.; Grady, K.C.; Allan, G.J.; Gehring, C.A.; Whitham, T.G.; Cushman, S.A.; Hultine, K.R. Adaptive Trait Syndromes along Multiple Economic Spectra Define Cold and Warm Adapted Ecotypes in a Widely Distributed Foundation Tree Species. Journal of Ecology 2021, 109, 1298–1318, doi:https://doi.org/10.1111/1365-2745.13557.
115. Schuster, A.-C.; Burghardt, M.; Riederer, M. The Ecophysiology of Leaf Cuticular Transpiration: Are Cuticular Water Permeabilities Adapted to Ecological Conditions? J Exp Bot 2017, 68, 5271–5279, doi:10.1093/jxb/erx321.
116. Billon, L.M.; Blackman, C.J.; Cochard, H.; Badel, E.; Hitmi, A.; Cartailler, J.; Souchal, R.; Torres-Ruiz, J.M. The DroughtBox: A New Tool for Phenotyping Residual Branch Conductance and Its Temperature Dependence during Drought. Plant Cell Environ 2020, 43, 1584–1594, doi:https://doi.org/10.1111/pce.13750.
117. Ochoa, M.E.; Henry, C.; John, G.P.; Medeiros, C.D.; Pan, R.; Scoffoni, C.; Buckley, T.N.; Sack, L. Pinpointing the Causal Influences of Stomatal Anatomy and Behavior on Minimum, Operational, and Maximum Leaf Surface Conductance. Plant Physiol 2024, 196, 51–66, doi:10.1093/plphys/kiae292.
118. Garen, J.C.; Michaletz, S.T. Temperature Governs the Relative Contributions of Cuticle and Stomata to Leaf Minimum Conductance. New Phytologist 2025, 245, 1911–1923, doi:https://doi.org/10.1111/nph.20346.
119. Pietsch, G.M.; Carlson, W.H.; Heins, R.D.; Faust, J.E. The Effect of Day and Night Temperature and Irradiance on Development of Catharanthus Roseus (L.) `Grape Cooler'. Journal of the American Society for Horticultural Science jashs 1995, 120, 877–881, doi:10.21273/JASHS.120.5.877.
120. Fotelli, M.; Rudolph, P.; Rennenberg, H.; Gessler, A. Irradiance and Temperature Affect the Competitive Interference of Blackberry on the Physiology of European Beech Seedlings. New Phytol 2005, 165, 453–462, doi:10.1111/j.1469-8137.2004.01255.x.
121. Magnani, F.; Grace, J.; Borghetti, M. Adjustment of Tree Structure in Response to the Environment under Hydraulic Constraints. Funct Ecol 2002, 16, 385–393, doi:https://doi.org/10.1046/j.1365-2435.2002.00630.x.
122. Addington, R.N.; Donovan, L.A.; Mitchell, R.J.; Vose, J.M.; Pecot, S.D.; Jack, S.B.; Hacke, U.G.; Sperry, J.S.; Oren, R. Adjustments in Hydraulic Architecture of Pinus Palustris Maintain Similar Stomatal Conductance in Xeric and Mesic Habitats. Plant Cell Environ 2006, 29, 535–545, doi:https://doi.org/10.1111/j.1365-3040.2005.01430.x.
123. Cochard, H.; Lemoine, D.; Dreyer, E. The Effects of Acclimation to Sunlight on the Xylem Vulnerability to Embolism in Fagus Sylvatica L. Plant Cell Environ 1999, 22, 101–108, doi:https://doi.org/10.1046/j.1365-3040.1999.00367.x.
124. Körner, C. Significance of Temperature in Plant Life. In Plant Growth and Climate Change; 2006; pp. 48–69 ISBN 9780470988695.
125. Menzel, A.; Sparks, T. Temperature and Plant Development: Phenology and Seasonality. In Plant Growth and Climate Change; 2006; pp. 70–95 ISBN 9780470988695.
126. Weih, M.; Liu, H.; Colombi, T.; Keller, T.; Jäck, O.; Vallenback, P.; Westerbergh, A. Evidence for Magnesium–Phosphorus Synergism and Co-Limitation of Grain Yield in Wheat Agriculture. Sci Rep 2021, 11, 9012, doi:10.1038/s41598-021-88588-8.

 doi:10.20944/preprints202504.1808.v1

127. Cossani, C.M.; Sadras, V.O. Chapter Six - Water–Nitrogen Colimitation in Grain Crops. In Advances in Agronomy; Sparks, D.L., Ed.; Academic Press, 2018; Vol. 150, pp. 231–274 ISBN 0065-2113.
128. Sperfeld, E.; Martin-Creuzburg, D.; Wacker, A. Multiple Resource Limitation Theory Applied to Herbivorous Consumers: Liebig's Minimum Rule vs. Interactive Co-Limitation. Ecol Lett 2012, 15, 142–150, doi:https://doi.org/10.1111/j.1461-0248.2011.01719.x.
129. Martin-StPaul, N.; Delzon, S.; Cochard, H. Plant Resistance to Drought Depends on Timely Stomatal Closure. Ecol Lett 2017, 20, 1437–1447, doi:https://doi.org/10.1111/ele.12851.
130. Lemoine, D.; Jacquemin, S.; Granier, A. Beech (Fagus Sylvatica L.) Branches Show Acclimation of Xylem Anatomy and Hydraulic Properties to Increased Light after Thinning. http://dx.doi.org/10.1051/forest:2002062 2002, 59.
131. Hacke, U.; Sauter, J.J. Vulnerability of Xylem to Embolism in Relation to Leaf Water Potential and Stomatal Conductance in Fagus Sylvatica f. Purpurea and Populus Balsamifera. J Exp Bot 1995, 46, 1177–1183, doi:10.1093/jxb/46.9.1177.
132. Aranda, I.; Cano, F.J.; Gascó, A.; Cochard, H.; Nardini, A.; Mancha, J.A.; López, R.; Sánchez-Gómez, D. Variation in Photosynthetic Performance and Hydraulic Architecture across European Beech (Fagus Sylvatica L.) Populations Supports the Case for Local Adaptation to Water Stress. Tree Physiol 2015, 35, 34–46, doi:10.1093/treephys/tpu101.
133. Likhachev, E. Dependence of Water Viscosity on Temperature and Pressure. Technical Physics 2003, 48, 514–515, doi:10.1134/1.1568496.
134. Kozlowski, T.T.; Pallardy, S.G. Vulnerability of Xylem to Embolism in Relation to Leaf Water Potential and Stomatal Conductance in Fagus Sylvatica f. Purpurea and Populus Balsamifera. Botanical Review 2002, 68, 270–334.
135. Santakumari, M.; Berkowitz, G.A. Chloroplast Volume: Cell Water Potential Relationships and Acclimation of Photosynthesis to Leaf Water Deficits. Photosynth Res 1991, 28, 9–20, doi:10.1007/BF00027172.
136. Rao, I.M.; Sharp, R.E.; Boyer, J.S. Leaf Magnesium Alters Photosynthetic Response to Low Water Potentials in Sunflower 1. Plant Physiol 1987, 84, 1214–1219, doi:10.1104/pp.84.4.1214.
137. Leuschner, C. Drought Response of European Beech (Fagus Sylvatica L.)—A Review. Perspect Plant Ecol Evol Syst 2020, 47, 125576, doi:10.1016/j.ppees.2020.125576.
138. Watson-Lazowski, A.; Cano, F.J.; Kim, M.; Benning, U.; Koller, F.; George-Jaeggli, B.; Cruickshank, A.; Mace, E.; Jordan, D.; Pernice, M.; et al. Multi-Omic Profiles of Sorghum Genotypes with Contrasting Heat Tolerance Connect Pathways Related to Thermotolerance. J Exp Bot 2024, erae506, doi:10.1093/jxb/erae506.
139. Aranda, I.; Rodríguez-Calcerrada, J.; Robson, T.M.; Cano, F.J.; Alté, L.; Sánchez-Gómez, D. Stomatal and Non-Stomatal Limitations on Leaf Carbon Assimilation in Beech (Fagus Sylvatica L.) Seedlings under Natural Conditions. For Syst 2012, 21, 405–417, doi:10.5424/fs/2012213-02348.
140. Rodríguez-Calcerrada, J.; Cano, F.; Valbuena, M.; Gil, L.; Aranda, I. Functional Performance of Oak Seedlings Naturally Regenerated across Microhabitats of Distinct Overstorey Canopy Closure. New For (Dordr) 2009, 39, 245–259, doi:10.1007/s11056-009-9168-1.
141. Osonubi, O.; Davies, W.J. Root Growth and Water Relations of Oak and Birch Seedlings. Oecologia 1981, 51, 343–350, doi:10.1007/BF00540904.
142. Kozlowski, T.; Pallardy, S. Acclimation and Adaptive Responses of Woody Plants to Environmental Stresses. The Botanical Review 2002, 68, 270–334, doi:10.1663/0006-8101(2002)068[0270:AAAROW]2.0.CO;2.
143. Aranda, I.; Gil, L.; Pardos, J. Seasonal Water Relations of Three Broadleaved Species (Fagus Sylvatica L., Quercus Petraea (Mattuschka) Liebl. and Quercus Pyrenaica Willd.) in a Mixed Stand in the Centre of the Iberian Peninsula. For Ecol Manage 1996, 84, 219–229, doi:https://doi.org/10.1016/0378-1127(96)03729-2.
144. Bucci, S.J.; Scholz, F.G.; Campanello, P.I.; Montti, L.; Jimenez-Castillo, M.; Rockwell, F.A.; Manna, L. La; Guerra, P.; Bernal, P.L.; Troncoso, O.; et al. Hydraulic Differences along the Water Transport System of South American Nothofagus Species: Do Leaves Protect the Stem Functionality? Tree Physiol 2012, 32, 880 – 893, doi:10.1093/treephys/tps054.
145. Rodríguez-Calcerrada Jesús and Sancho-Knapik, D. and M.-S.N.K. and L.J.-M. and M.N.G. and G.-P.E. Drought-Induced Oak Decline—Factors Involved, Physiological Dysfunctions, and Potential Attenuation

 doi:10.20944/preprints202504.1808.v1

by Forestry Practices. In Oaks Physiological Ecology. Exploring the Functional Diversity of Genus Quercus L.; Gil-Pelegrín Eustaquio and Peguero-Pina, J.J. and S.-K.D., Ed.; Springer International Publishing: Cham, 2017; pp. 419–451 ISBN 978-3-319-69099-5.

146. Munné-Bosch, S.; Alegre, L. Die and Let Live: Leaf Senescence Contributes to Plant Survival under Drought Stress. Functional Plant Biology 2004, 31, 203–216.
147. WARREN, C.R.; ARANDA, I.; CANO, F.J. Responses to Water Stress of Gas Exchange and Metabolites in Eucalyptus and Acacia Spp. Plant Cell Environ 2011, 34, 1609–1629, doi:https://doi.org/10.1111/j.1365-3040.2011.02357.x.
148. Aranda, I.; Sánchez-Gómez, D.; Cadahía, E.; Fernández de Simón, B. Ecophysiological and Metabolic Response Patterns to Drought under Controlled Condition in Open-Pollinated Maternal Families from a Fagus Sylvatica L. Population. Environ Exp Bot 2018, 150, doi:10.1016/j.envexpbot.2018.03.014.
149. López, R.; Rodríguez-Calcerrada, J.; Gil, L. Physiological and Morphological Response to Water Deficit in Seedlings of Five Provenances of Pinus Canariensis: Potential to Detect Variation in Drought-Tolerance. Trees 2009, 23, 509–519, doi:10.1007/s00468-008-0297-5.
150. Limousin, J.-M.; Roussel, A.; Rodríguez-Calcerrada, J.; Torres-Ruiz, J.M.; Moreno, M.; Garcia de Jalon, L.; Ourcival, J.-M.; Simioni, G.; Cochard, H.; Martin-StPaul, N. Drought Acclimation of Quercus Ilex Leaves Improves Tolerance to Moderate Drought but Not Resistance to Severe Water Stress. Plant Cell Environ 2022, 45, 1967–1984, doi:https://doi.org/10.1111/pce.14326.
151. Fanourakis, D.; Heuvelink, E.; Carvalho, S.M.P. A Comprehensive Analysis of the Physiological and Anatomical Components Involved in Higher Water Loss Rates after Leaf Development at High Humidity. J Plant Physiol 2013, 170, 890–898, doi:https://doi.org/10.1016/j.jplph.2013.01.013.
152. Grime, J.P.; Mackey, J.M.L. The Role of Plasticity in Resource Capture by Plants. Evol Ecol 2002, 16, 299–307, doi:10.1023/A:1019640813676.
153. Haaland, T.R.; Wright, J.; Ratikainen, I.I. Individual Reversible Plasticity as a Genotype-level Bet-hedging Strategy. J Evol Biol 2021, 34, 1022–1033, doi:10.1111/jeb.13788.
154. Nielsen, M.E.; Papaj, D.R. Why Study Plasticity in Multiple Traits? New Hypotheses for How Phenotypically Plastic Traits Interact during Development and Selection. Evolution (N Y) 2022, 76, 858–869, doi:10.1111/evo.14464.
155. Schlichting, C.D.; Pigliucci, M. Phenotypic Evolution: A Reaction Norm Perspective.; Sinauer Associates Incorporated: Sunderland, 1998; ISBN 9780878937998.
156. Van Buskirk, J.; Steiner, U.K. The Fitness Costs of Developmental Canalization and Plasticity. J Evol Biol 2009, 22, 852–860, doi:10.1111/j.1420-9101.2009.01685.x.
157. Robson, T.; Rodríguez-Calcerrada, J.; Sánchez-Gómez, D.; Aranda, I. Summer Drought Impedes Beech Seedling Performance More in a Sub-Mediterranean Forest Understory than in Small Gaps. Tree Physiol 2009, 29, 249–259, doi:10.1093/treephys/tpn023.
158. Grossiord, C.; Buckley, T.N.; Cernusak, L.A.; Novick, K.A.; Poulter, B.; Siegwolf, R.T.W.; Sperry, J.S.; McDowell, N.G. Plant Responses to Rising Vapor Pressure Deficit. New Phytologist 2020, 226, 1550–1566, doi:https://doi.org/10.1111/nph.16485.
159. Aranda, I.; Gil, L.; Pardos, J. Water Relations and Gas Exchange in Fagus Sylvatica L. and Quercus Petraea (Mattuschka) Liebl. In a Mixed Stand at Their Southern Limit of Distribution in Europe. Trees 2000, 14, 344–352, doi:10.1007/s004680050229.
160. Mas, E.; Cochard, H.; Deluigi, J.; Didion-Gency, M.; Martin-StPaul, N.; Morcillo, L.; Valladares, F.; Vilagrosa, A.; Grossiord, C. Interactions between Beech and Oak Seedlings Can Modify the Effects of Hotter Droughts and the Onset of Hydraulic Failure. New Phytologist 2024, 241, 1021–1034, doi:https://doi.org/10.1111/nph.19358.
161. Schneider, C.A.; Rasband, W.S.; Eliceiri, K.W. NIH Image to ImageJ: 25 Years of Image Analysis. Nat Methods 2012, 9, 671–675, doi:10.1038/nmeth.2089.
162. Holland, N.; Richardson, A. Stomatal Length Correlates with Elevation of Growth in Four Temperate Species†. Journal of Sustainable Forestry 2009, 28, 63–73, doi:10.1080/10549810802626142.

 doi:10.20944/preprints202504.1808.v1

163. Araus, J.L.; Febrero, A.; Vendrell, P. Epidermal Conductance in Different Parts of Durum Wheat Grown under Mediterranean Conditions: The Role of Epicuticular Waxes and Stomata. Plant Cell Environ 1991, 14, 545–558, doi:https://doi.org/10.1111/j.1365-3040.1991.tb01525.x.
164. Robichaux, R.H. Variation in the Tissue Water Relations of Two Sympatric Hawaiian Dubautia Species and Their Natural Hybrid. Oecologia 1984, 65, 75–81.
165. TYREE, M.T.; HAMMEL, H.T. The Measurement of the Turgor Pressure and the Water Relations of Plants by the Pressure-Bomb Technique. J Exp Bot 1972, 23, 267–282, doi:10.1093/jxb/23.1.267.
166. Dreyer, E.; Bousquet, F.; Ducrey, M. Use of Pressure Volume Curves in Water Relation Analysis on Woody Shoots: Influence of Rehydration and Comparison of Four European Oak Species. Ann. For. Sci. 1990, 47, 285–297.
167. KUBISKE, M.E.; ABRAMS, M.D. Pressure-Volume Relationships in Non-Rehydrated Tissue at Various Water Deficits. Plant Cell Environ 1990, 13, 995–1000, doi:https://doi.org/10.1111/j.1365-3040.1990.tb01992.x.
168. Brodribb, T.J.; Holbrook, N.M. Stomatal Protection against Hydraulic Failure: A Comparison of Coexisting Ferns and Angiosperms. New Phytologist 2004, 162, 663–670, doi:https://doi.org/10.1111/j.1469-8137.2004.01060.x.
169. Al-Salman, Y.; Cano, F.J.; Mace, E.; Jordan, D.; Groszmann, M.; Ghannoum, O. High Water Use Efficiency Due to Maintenance of Photosynthetic Capacity in Sorghum under Water Stress. J Exp Bot 2024, 75, 6778–6795, doi:10.1093/jxb/erae418.
170. López, R.; Nolf, M.; Duursma, R.A.; Badel, E.; Flavel, R.J.; Cochard, H.; Choat, B. Mitigating the Open Vessel Artefact in Centrifuge-Based Measurement of Embolism Resistance. Tree Physiol 2019, 39, 143–155, doi:10.1093/treephys/tpy083.
171. Robson, T.M.; Sánchez-Gómez, D.; Cano, F.J.; Aranda, I. Variation in Functional Leaf Traits among Beech Provenances during a Spanish Summer Reflects the Differences in Their Origin. Tree Genet Genomes 2012, 8, 1111–1121, doi:10.1007/s11295-012-0496-5.
172. Scholz, A.; Klepsch, M.; Karimi, Z.; Jansen, S. How to Quantify Conduits in Wood? Front Plant Sci 2013, 4.
173. Valladares, F.; Sánchez-Gómez, D.; Zavala, M.A. Quantitative Estimation of Phenotypic Plasticity: Bridging the Gap between the Evolutionary Concept and Its Ecological Applications. Journal of Ecology 2006, 94, 1103–1116, doi:https://doi.org/10.1111/j.1365-2745.2006.01176.x.